GERMAN - MONGOLIAN INSTITUTE
FOR RESOURCES AND TECHNOLOGY

The present work was submitted to
the German-Mongolian Institute of Resources and Technology

TRACER-BASED INVESTIGATION OF GROUNDWATER FLOW AND CONNECTIVITY IN FRACTURED AQUIFERS

Bachelor's Thesis

By

TEMUULEN Delgersuuri

Study program: Environmental Engineering

Student ID: B2200534

1st Supervisor: Dr. Ariuntuya Tserendorj

2nd Supervisor: Dr. Prof. Traugott Scheytt

Ulaanbaatar/Nalaikh

2026

Statutory Declaration

Delgersuuri, Temuulen — B2200534

Last Name, First Name — Student ID Number

I hereby affirm in lieu of an oath that I provided the submitted bachelor thesis

TRACER-BASED INVESTIGATION OF GROUNDWATER FLOW AND CONNECTIVITY IN FRACTURED AQUIFERS

I did not use any sources other than those stated. In case that the work is additionally submitted on a data medium, I declare that the written and the electronic form are completely identical. The work was not submitted in the same or similar form to any examination authority.

Ulaanbaatar, 29/06/2026

Place, Date

Signature

Abstract

The fluorescence tracer uranine is frequently applied to groundwater studies, but its behavior in fractured crystalline aquifers is still not well constrained since apparent tracer losses may be due to actual sorption on rock surfaces or changes in fluorescence intensity with temperature.

The purpose of this study was to measure the temperature dependency of uranine in solution within water-groundwater mixtures as well as in batch contact with crushed gneiss from the fractured aquifer system of Freiberg (Germany), to separate the true sorption behavior of uranine onto the rock from apparent uranine concentration changes induced by temperature-dependent fluorescence quenching.

Batch reactor experiments were performed with aqueous solutions of groundwater only, groundwater and uranine, and groundwater, uranine, and gneiss at initial uranine concentrations of 0.5, 5, 20, and 50 µg/L and at temperatures of 10, 25, and 55 °C.

Triplicate reactors were quantified using temperature-specific calibration curves prepared in the same groundwater matrix as the samples. For each temperature, calibration standards consisted of Freiberg groundwater containing known uranine concentrations but no gneiss, so that both matrix effects and temperature-dependent fluorescence quenching were incorporated into the concentration calculation

Correcting for this fluorescence–temperature dependence, uranine exhibits no detectable sorption at concentrations of 0.5 and 5 µg/L at any temperature within the limits of analytical detection. Weak sorption is detectable at concentrations of 20 µg/L, and higher still at 50 µg/L, with up to several tens of percent sorption observed in some cases. Temperature showed only a modest and non-systematic effect on sorption, with some datasets even showing higher sorption at 10 °C relative to 25 °C or 55 °C.

Overall, these data suggest that uranine is likely to behave as a conservative tracer under the chemical conditions presented here at concentrations commonly applied in the field, but that non-conservative behavior may be important at higher concentrations and should be considered in tracer tests in crystalline aquifers.

Keywords: Uranine; fractured gneiss aquifer; sorption; thermal quenching; fluorescence calibration; batch equilibrium; water-rock interaction.`

Acknowledgements

First of all, I would like to thank my supervisor, Dr. Ariuntuya Tserendorj, for her encouragement and helpful comments during all periods of this thesis. Her support, valuable criticism, and patience helped me a lot during every phase of work.

I would like to thank Prof. Dr Traugott Scheytt, Chair of Hydrogeology and Hydrochemistry at Technische Universität Bergakademie Freiberg (TUBAF) very much for his warm welcome and the opportunity to complete this research in his group. Many thanks to him for providing the academic conditions to implement this thesis work.

I am deeply grateful to Frank Schenker (TUBAF) for his patient guidance and practical help, and constant support during experiments and the completion of this thesis. Frank helped me a lot with solving practical issues during the work in the laboratory and allowing the work to flow efficiently.

Thanks to Rebekka Wiedener and Tobias Lotter (TUBAF) for their help, advice and support during the work on the project. They assisted me during the experiments and while working on completing the thesis.

Finally, I would like to thank the laboratory assistants of the Hydrogeology and Hydrochemistry Department for providing materials, equipment, and working conditions for conducting experiments. Their cooperation and readiness to help allowed the creation of the professional and organized atmosphere necessary for the laboratory work.

Thank you to my parents for their continuous support, understanding, and encouragement during all my studying years. Without their confidence in me and constant support, it would not have been possible to complete this work.

Contents

1. Introduction 1
1.1 Background and Rationale 1
1.2 Aim and Objectives 1
2. State of the Art 2
2.1 Fluorescent dyes and uranine in hydrology 2
2.2 Conditional conservativity of fluorescent dyes 2
2.3 Controls on sorption and retention in soils and unconsolidated sediments 3
2.4 Sorption and retention in consolidated aquifer media 4
2.5 Temperature, thermal quenching, and matrix effects on uranine detection 5
2.6 Crystalline and gneiss aquifers: tracer work and knowledge gaps 7
3. Problem statement 9
4. Materials and Methods 10
4.1 Study area and material preparation 10
4.2 Experimental design 11
4.2.1 Batch reactor setup and handling 12
4.3 Analytical methods 13
4.3.1 Fluorescence spectroscopy 14
4.3.2 Ion chromatography and ICP-OES 15
4.3.3 Field parameters and carbonate hardness 16
4.4 Data treatment 17
4.4.1 Calculation of ionic strength, hardness, and alkalinity 17
4.4.2 Calculation of Release per Unit Mass 17
4.4.3 Calculation of sorption 18
4.4.4 Statistical analysis 19
5. Results 21
5.1 Hydrochemical Characterization 21
5.1.1 Long-term Field Monitoring and Baseline Groundwater Chemistry 21
5.1.2 Ionic strength, hardness, alkalinity 22
5.1.3 Experimental Waters and Charge Balance 23
5.1.4 Field Parameters in WT and WTG Reactors 24
5.2 Element Release from Gneiss in Batch Reactors 25
5.2.1 Major-Ion Behavior in WT and WTG Systems 25
5.3 Fluorescence Calibration and Temperature Dependence of Uranine 26
5.3.1 Temperature-Specific Calibration Curves 27
5.4 Uranine Sorption onto Gneiss 28
5.4.1 Sorbed Amounts and Distribution Coefficients 28
5.4.2 Statistical Evaluation and Minimum Detectable Sorption 29
5.4.3 Factorial effects of concentration and temperature on uranine sorption 29

5.5 Integrated Assessment of Uranine Behavior and Element Release 31
6. Discussion 32
6.1 Interpretation of Release Patterns 32
6.2 Temperature effects on fluorescence versus sorption 32
6.3 Comparison with the wider tracer literature 33
6.4 Implications for field tracer tests 34
6.5 Interpretation of concentration and temperature effects on sorption 35
6.6 Uncertainty and analytical limitations 36
6.7 Contribution to literature 38
7. Future Work 39
8. Conclusion 40
References 41
Appendix A 43
A.1 Mean (± 1 SD) anion concentrations in batch reactor samples — Ion Chromatography (IC) 43
A2. Mean (± 1 SD) major cation concentrations in batch reactor samples — Ion Chromatography (IC) 44
A3. Mean (± 1 SD) trace element concentrations in batch reactor samples — ICP-OES (µg/L) 45
Appendix B 47
B.1 Full batch-sorption dataset 47
Appendix C 51
C.1 Field parameters in WT and WTG reactors 51

List of Figures

Figure 1 Sampling process from the test site 10
Figure 2 Initial stock solutions 11
Figure 3 Schematic of batch reactor systems (generated using Gemini AI) 12
Figure 4 Reactors in a thermocabinet 13
Figure 5 Reactors after 24h in an orbital shaker 13
Figure 6 Reactors containing rock media are being centrifuged 14
Figure 7 IC samples before testing 15
Figure 8 EC, pH, and temperature measurement using a multimeter 16
Figure 9 Titration process to test carbonate hardness 16
Figure 10 Electrical conductivity in WT and WTG reactors at all tested temperatures and nominal uranine concentrations. 25
Figure 11 Major cation concentrations in the original groundwater and its temperature treatment variants without gneiss. 25
Figure 12 Temperature-specific calibration curves for uranine fluorescence at 10 °C, 25 °C, and 55 °C. 27
Figure 13 Sorption versus nominal uranine concentration, with separate curves for 10 °C, 25 °C, and 55 °C 30

List of Tables

Table 1 Major-ion composition of groundwater from the Freiberg gneiss aquifer. 21
Table 2 Field parameters of groundwater from the Freiberg gneiss aquifer. 22
Table 3 Measured cation and anion concentrations (mg L^{-1}) 23
Table 4 Cation and anion charge-balance 24
Table 5 Mean uranine sorption (q, µg g^{-1}) 29
Table 6 Two-factor ANOVA table for uranine sorption (q) with concentration, temperature, and their interaction as fixed factors. 30

1. Introduction

1.1 Background and Rationale

Fractured crystalline aquifers are a primary groundwater resource worldwide, but are difficult to characterize using standard hydrogeological approaches due to their intrinsic heterogeneity [1]. Among the methods available to probe directly flow paths, velocities, and transport properties, tracer tests with fluorescent dyes have become an essential data acquisition technique for complex systems such as crystalline aquifers. Uranine (sodium fluorescein) is one of the most frequently used fluorescent tracers because of its intense fluorescence signal, low detection limits, and low toxicity [3]. In groundwater tracer tests, uranine is commonly considered a “quasi-conservative” tracer, expected to follow the advective flow path without appreciable retardation or reaction with the matrix [3–5].

This conservativity is conditional because sorption to rock surfaces or fracture-filling material can reduce tracer recovery, while temperature-dependent fluorescence quenching can alter the measured signal independently of concentration [4–6]. Uranine, like any other dye, is affected by fluorescence thermal quenching. Distinguishing apparent tracer loss from thermal quenching and true loss of mass from sorption is crucial to avoid erroneous interpretation of field data sets [3,5].

1.2 Aim and Objectives

This thesis aims to determine the temperature-dependent behavior of uranine in fractured gneiss aquifer material at the test site in Freiberg using laboratory experiments. The focus will be set on distinguishing physical processes of tracer retention (i.e., sorption) from technical effects (i.e., thermal quenching). Therefore, empirical data will be provided to support the interpretation of uranine tracer tests in crystalline rocks.

Thesis goals are:

- To establish a precise calibration curve linking uranine concentration to fluorescence intensity within the normal environmental range of both concentration and temperature for Freiberg gneiss groundwater.

- To characterize the temperature and initial concentration dependence of uranine sorption onto gneiss using batch equilibrium experiments.
- To distinguish quantitatively between mass loss due to sorption and mass loss due to changes in fluorescence signal caused by thermal quenching.

2. State of the Art

2.1 Fluorescent dyes and uranine in hydrology

Fluorescent dyes are routinely used to delineate catchments, determine flow paths, and quantify velocities and dispersion in karst and fractured aquifers, where direct observation of flow would otherwise be impossible [2]. Karst environments are the classic example, where uranine is often the tracer of first choice. Its high water solubility, low toxicity, and extremely low detection limit (quoted as ~0.005 μg L^{-1} in some sources [2, 8] allow practitioners to use small injection masses and still record breakthrough curves that are clear enough to interpret.

Leibundgut et al. [8] write extensively on fluorescent tracers and identify uranine as the "dominant" dye based on its much higher fluorescence intensity compared to other dyes, and its very low detection limit achievable under optimal conditions. In this work, the same authors summarize the key properties of several commonly used dyes, including excitation/emission wavelengths, achievable detection limits, and relative fluorescence yields. They also classify each dye according to its sorption behavior (uranine is classed as "very good," meaning low sorption) and toxicological hazard. This clearly explains uranine's widespread adoption as a near-conservative tracer in porous, fissured, and karst aquifers [8].

2.2 Conditional conservativity of fluorescent dyes

On closer inspection, however, classical tracer methodology, as summarized by Leibundgut et al. [8], shows that the conservativity of fluorescent dyes is conditional. Dye behavior is influenced by pH, temperature, light, sorption processes, and chemical or biological stability. These factors can become important in certain environments, such as acidic soils, peatlands, or highly mineralized waters. Goldscheider et al. [2] specifically address the use of fluorescent dyes in karst hydrogeology, noting that uranine performs

well across many carbonate environments. However, they do point out that these dyes might not accurately reflect water movement or could be significantly slowed down in environments that are high in organic matter or acidic, suggesting that other tracers like naphthionate, tinopal, or rhodamines might be more suitable in such cases.

2.3 Controls on sorption and retention in soils and unconsolidated sediments

Recent laboratory batch experiments have begun to untangle the controls on fluorescent tracer retention in soils and unconsolidated sediments. Working with uranine (UR) and sulforhodamine B (SRB), Bork et al. [2] conducted experiments using a sandy sediment, and both topsoil and subsoil with different amounts of organic carbon. They found strong increases in sorption with decreasing pH for both dyes, which were much more pronounced for uranine; greater UR sorption in the organic-rich topsoil than in the subsoil at pH 5.5 and 6.5. The difference between these soils became negligibly small at pH 7.5, implying that organic matter influences sorption behavior most in acidic environments; enhanced sorption of both dyes upon addition of montmorillonite to a sandy sediment. Sorption was high (~80 %) for both UR and SRB at ~3–4 % added clay, corresponding to a near-complete removal from solution.

Opposite effects of organic carbon content: increasing organic carbon content caused increased sorption of UR, but decreased sorption of SRB, reflecting different mechanisms of interaction with organic matter. This is also evident in the reported K_d values, where K_d represents the equilibrium distribution coefficient between the solid and aqueous phases, and higher values indicate stronger sorption [8, 10].

The authors report K_d values for uranine of up to ~73 $L\ kg^{-1}$ in acidic, organic-rich soils (pH 5.5), but much lower (often zero) values in neutral, sandy sediments. This highlights again that fluorescent dyes can exhibit behavior from conservative to strongly retarded, depending on the geological matrix [2].

The tracer monograph by Leibundgut et al. [3] reports broadly similar behaviour. They summarize batch and column studies, which demonstrate that K_d for uranine is typically low in sandy, low-OC matrices but increases to several $L\ kg^{-1}$ in clays and organic-rich soils, while eosine and many rhodamines are much more strongly sorbed. Uranine is

therefore recommended for use as a conservative tracer in porous groundwater where the aquifer material is known to have low organic carbon content. Its use in humic soil or environments with acidic conditions should be avoided [3].

These observations agree with wider literature on organic-contaminant sorption to soils and aquifer materials. Abdul and Gibson [4] measured linear adsorption isotherms for six PAHs (polycyclic aromatic hydrocarbons) across two aquifer materials, demonstrating that adsorption at low aqueous concentrations could be modelled using the linear equation $S_e = K_d \times C_e$. Spanning the two materials, K_d values differed by up to an order of magnitude. They also note that sorption is predominantly controlled by organic carbon content, and that batch experiment results can depend on sorbent mass, phase separation, and equilibration methods [4]. The latter point is now common practice in dye sorption experiments.

2.4 Sorption and retention in consolidated aquifer media

For consolidated media, batch and diffusion experiments were used by Sabatini [4] to study sorption and intraparticle diffusion of various fluorescent dyes within sandstone and other aquifer rocks. Although they are not reproduced here, they found that cationic dyes such as rhodamine exhibit strong sorption; anionic dyes such as uranine show low, but non-zero sorption in clean, low-OC sandstone; sorption increases considerably in the presence of clay coatings or organic films within the rock matrix, and intrapore diffusion into microporous grains may control kinetics and lead to strong tailing of breakthrough curves even if sorbed equilibrium amounts are low.

This is confirmed by the studies conducted by Vaitl and Wohnlich [7], in which batch tests with uranine, amidorhodamine G, and Tinopal CBS-X were performed on sandstone, claystone, and limestone [4,7]. They report almost conservative behavior of uranine in both sandstones and limestones (very low K_d values and < ~2–5 % removal at high aqueous concentrations); considerably higher sorption of uranine in claystone (up to 70%) removal at similar concentrations, K_d values around one order of magnitude higher; extremely strong sorption of tinopal CBS-X, particularly within claystone, making it generally unfit as a conservative tracer in these media.

From kinetic experiments, they conclude that sorption behavior can often be described by pseudo-first-order equations and that equilibrium is not necessarily reached after 24h in

mechanically crushed rock samples, partly due to continuous particle breakage, which increases reactive surface area [4,7]. Continuous flow through intact rock discs better reflects actual field conditions, they maintain, without any need for crushing [4,7].

The OECD Test Guideline 106 (Organisation for Economic Co-operation and Development) gives general guidance on batch adsorption–desorption studies. It recommends determining K_d values (and organic-carbon-normalized K_d values) for chemicals over representative soils, highlighting pH, organic carbon content, clay content, and cation-exchange capacity as major controlling factors [5]. It points out that linear K_d values are sufficient to describe sorption at low concentrations for most chemicals and have therefore found wide use as (relative) mobility indicators in leaching classification systems. Details like soil/solution ratio, equilibration time, or analytical method accuracy are discussed [5].

Crystalline rocks and gneiss are significantly under-studied regarding dye sorption. Available batch studies mainly consider soils, unconsolidated sediments, sandstones, limestones, and model sorbents such as clays or humic substances [4,6,7]. Quantitative dye–gneiss data are currently lacking, despite crystalline aquifers being relatively common and often utilized for drinking water extraction.

2.5 Temperature, thermal quenching, and matrix effects on uranine detection

The fluorescence signal used to quantify uranine depends on both concentration and environmental conditions. According to basic principles of fluorescence theory, increased temperature should favor non-radiative decay processes and decrease quantum yield and fluorescence intensity (“thermal quenching”) [11]. Baker [12] found pronounced temperature dependences for fluorescence from dissolved organic matter (DOM) in river and wastewater samples measured across 10–45 °C. All major fluorophore “peaks” showed systematic decreases in intensity with temperature, including those attributed to tryptophan-like and fulvic-like material. Reductions in fluorescence intensity were in the range of 18–50 % across the temperature range studied [12]. Critically, excitation and emission wavelengths did not change with temperature, suggesting the DOM composition remained constant and only quantum yield was affected [12]. Blaen et al. [5] directly measured the impacts of temperature and turbidity on uranine fluorescence and that of a reactive dye couple (resazurin/resorufin) using a field-based multitracer stream

experiment. Results showed that fluorescence readings taken in situ with a field fluorometer systematically underestimated tracer concentrations compared to laboratory spectrofluorometry by ~20–37 %. Discrepancies increased with turbidity and temperature. Recalibration of the field fluorometer using laboratory samples revealed pronounced, tracer-specific temperature dependences wherein fluorescence intensity decreased log-linearly with increasing temperature for uranine and resorufin. Effects were amplified at a lower concentration. The effects of turbidity were linear for both tracers, causing both positive biases at low turbidity (resulting from scattering of the excitation light) and negative biases at higher turbidity.

Correction functions were developed to account for temperature and turbidity effects, and agreement between in situ and laboratory data was shown to improve when applying these functions. The authors note that environmental variability, if left uncorrected, can introduce substantial uncertainty to tracer breakthrough curves, particularly in multitracer experiments.

Detection of Na-fluorescein in mine waters has revealed other important matrix effects. Weidner et al. [13] studied detection and noted three important complications when working with acidic, metal-rich mine waters. They found that eosine interference in multitracer applications as spectra are essentially identical; losing uranine fluorescence upon precipitation of minerals from samples during buffering or neutralization; enhanced quenching by high concentrations of Fe and Mn. They demonstrated that utilizing a second fluorescence maximum of uranine available at pH ≈ 1.5, along with a different excitation wavelength (~438 nm), allowed some of these issues to be overcome, aiding detectability in these extreme matrices.

Extreme concentration can introduce self-quenching effects as well. Luchowski et al. [14] measured uranine in solids at high concentrations by depositing it within polyvinyl alcohol films. They observed that at concentrations of 0.18–0.54 M, the fluorescence lifetime decreased to 7–10 ps while the quantum yield dropped to only ~0.002. Despite this extreme self-quenching, intensity decay remained homogeneous and was described by a single lifetime [14]. These self-quenched samples were suggested to be useful as ultra-short-lifetime fluorescent standards to measure instrument response functions in time-resolved fluorescence experiments. The work highlighted the role of exciton migration and dye–dye energy transfer dominating the photophysics of uranine fluorescence at high concentrations [14]. While concentrations this high are unlikely to

be used for hydrological tracing applications, self-quenching may still be an issue at lower concentrations.

Effects of salinity have also been described. Magal et al. [15] examined five dyes under highly saline conditions using natural groundwaters and synthetic waters of salinities equivalent to Dead Sea brine. They found that SRB and eosine strongly sorbed to both pure minerals and natural sediment samples, ruling them out as truly conservative tracers under saline conditions; uranine and pyranine exhibited salinity-dependent sorption as well, resulting in moderate to strong retention from Dead Sea water, particularly for clayey sediments; naphthionate showed negligible sorption across all cases and was proposed to be the most conservative tracer dye in both fresh and saline groundwater.

Additional work from this study showed that the distribution coefficient of uranine in Dead Sea water depended on the sediment-to-solution ratio and sediment grain size. Higher K_d were obtained at lower sediment loading rates and with finer sediment grain sizes. This phenomenon could explain some of the disparity between studies measuring the sorption of uranine to natural sediments.

2.6 Crystalline and gneiss aquifers: tracer work and knowledge gaps

Crystalline-rock aquifers, and particularly gneiss, form important groundwater resources in many regions. In the Freiberg area (Saxony, Germany), the main aquifer is a fractured gneiss of the Erzgebirge basement, where groundwater flow is largely confined to discrete fracture zones and weathered horizons [16]. Packer tests, geophysical logs, and hydraulic modelling indicate strong heterogeneity, with flow predominantly in a limited number of conductive fractures and negligible flow in the intact matrix [16].

Abdelaziz and Merkel [16] applied analytical (MLU) and numerical (ANSYS/FLOTRAN) models to interpret packer tests in this fractured gneiss, concluding that hydraulic conductivity is highly variable with depth and that non-fractured gneiss is essentially impermeable; groundwater flow is focused in a few major fracture zones. Follow-up work used tracer tests with NaCl under natural gradient conditions, combined with MODFLOW–MT3DMS transport modelling and inverse calibration (UCODE), to estimate effective hydraulic conductivity, porosity, and immobile-porosity parameters [1]. These studies showed that late-time tailing in breakthrough curves can be explained

by dual-porosity behavior and that immobile porosity plays an important role in solute exchange between fractures and matrix [1].

A Lattice Boltzmann model was subsequently used to simulate NaCl transport through a fracture zone at the same site, reproducing measured breakthrough curves reasonably well and demonstrating the potential of pore-scale methods to capture heterogeneous flow and transport in fractured gneiss [17]. However, all these tracer experiments used conservative salts and nonquantified sorption or retention of fluorescent dyes.

Hence, although the hydraulic properties of the Freiberg fractured gneiss aquifer are known in great detail, only scarce site-specific published information could be found about uranine sorption on gneiss fracture-wall material, temperature-dependent fluorescence of uranine in Freiberg groundwater, and the combined impact of water-rock interaction and temperature on apparent uranine recovery.

Given the evidence from soils, sediments, sandstones, and limestones that fluorescent tracers can be measurably retarded by sorption and intraparticle diffusion [6], and the clear temperature and matrix effects on uranine detection [5,13], it is unlikely that uranine is perfectly conservative in fractured gneiss aquifers. Yet the absence of site-specific batch sorption and fluorescence–temperature data for gneiss represents a significant gap in the current state of the art.

3. Problem statement

Numerous studies have investigated one or both factors affecting uranine behavior across diverse environmental settings. However, our review of the state of the art highlighted two remaining gaps in knowledge at the intersection of tracer hydrology and crystalline rock hydrogeology [3–6]:

Crystalline rocks are largely understudied compared to soils, unconsolidated sediments, and porous sedimentary rocks such as sandstone or limestone in systematic batch experiments that quantify uranine sorption coefficients [4,6,7]. Uranine sorption onto crystalline rocks, and particularly gneiss, which forms widespread aquifers worldwide, is unknown [4,6,7].

Temperature effects on fluorescence intensity (“thermal quenching”) and sorption have been studied separately. Very few studies have considered both phenomena simultaneously and quantified their respective impacts on apparent tracer recovery in the fractured rock setting relevant to a crystalline aquifer system [1–5].

4. Materials and Methods

All procedures are described in sufficient detail to allow full replication of the batch experiments and associated analytical measurements.

4.1 Study area and material preparation

Aquifer material and groundwater were obtained from the test site in Freiberg, Saxony, Germany. The Freiberg experimental field site is a fractured crystalline rock aquifer that has been the focus of numerous hydraulic and tracer tests, which is situated at 50.9252384° N, 13.3306216° E (EPSG:4326, WGS 84).

Groundwater and drill cuttings were sampled from an observation well approximately 79 m in depth, which passes through hydraulically active fracture networks within the gneiss. To remain consistent with examining tracer–rock interactions that occur under conditions that are as close to in situ aquifer conditions as possible, only bulk partitioning of the tracer to the gneiss lithology is considered, rather than mineral-specific sorption.

Sample groundwater was obtained for all experiments on 15 December 2025 by pumping from the observation well, as shown in Figure 1.



Figure 1 Sampling process from the test site

Gneiss samples were oven dried at 105 °C for a 24 hours, and mechanically sieved to < 2 mm. No washing or other chemical treatment of the gneiss was conducted. Thus, any

surface coating remains intact (i.e., weathering products, secondary minerals, etc.). This was done to simulate water–rock interactions that happen naturally in the subsurface.

Uranine (sodium fluorescein, CAS 518-47-8) of analytical reagent grade was utilized as the fluorescent tracer dye. A single stock solution was created at the onset of experimentation by dissolving a precisely weighed amount of uranine powder into groundwater to produce a concentrated solution of uranine in groundwater. This stock solution was kept in an amber colored glass bottle wrapped in aluminum foil (see Figure 5) and stored at room temperature to prevent photodegradation (see Figure 2). The stock was made readily accessible for future use throughout the course of the experimental study.

4.2 Experimental design

Working solutions at the nominal concentrations of 0.5, 5, 20, and 50 µg/L were made by diluting the stock solution stepwise using the same groundwater.



Figure 2 Initial stock solutions

Three batch systems were prepared for each temperature/concentration combination:

- Blank (B): groundwater only, no uranine, no gneiss — control to track background fluorescence, water chemistry baseline, and instrument drift.

- Water and tracer (WT): groundwater and uranine at target concentration, no gneiss — to measure uranine fluorescence at each temperature in the absence of rock and generate temperature-specific calibration curves.
- Water, tracer, and gneiss (WTG): groundwater and uranine at target concentration to measure sorption and water–rock interactions.

The three reactor types used in this study are illustrated schematically in Figure 3. Three temperatures were chosen: 10, 25, and 55 °C. These approximate cold shallow groundwater conditions, typical laboratory/temperate aquifer conditions, and provide an upper bound, respectively. Three replicate batch reactors were prepared for each temperature–concentration–system (B, WT, WTG; 0.5, 5, 20, 50 µg/L) combination, providing triplicate data for statistical comparison. Contact time was 24 h for all reactors, which was expected to be sufficient for uranine sorption onto gneiss under these conditions to reach apparent equilibrium, and is in accordance with OECD guidance on batch equilibrium experiments. After 24 hours of equilibration, reactors were removed from the orbital shaker, as shown in Figure 4.

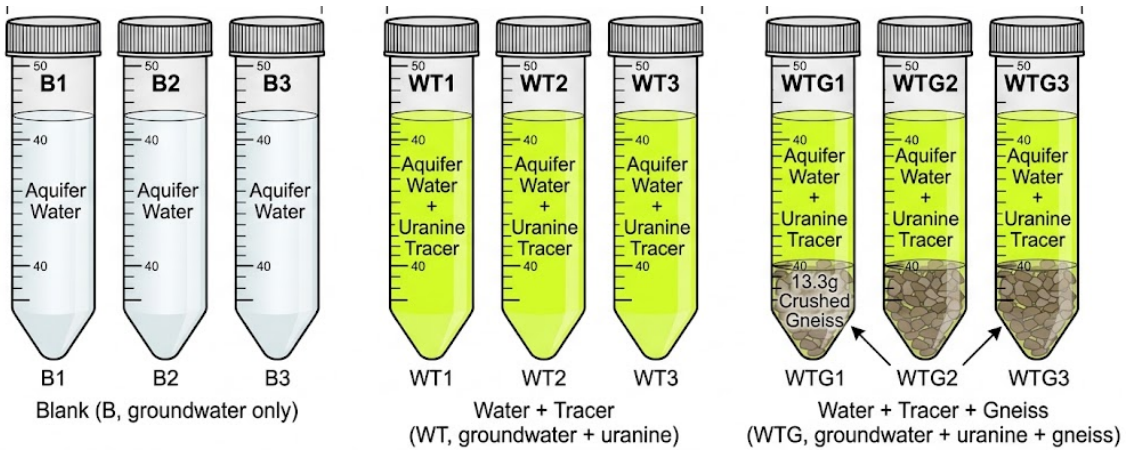


Figure 3 Schematic of batch reactor systems (generated using Gemini AI)

4.2.1 Batch reactor setup and handling

50 mL polypropylene (PP) tubes were used as batch reactors in all experiments. The tubes were precleaned and labelled with the full experiment code. For WTG reactors, 13.3 ± 0.01 g of gneiss was weighed into each tube (solid to solution ratio of 1:3). For all reactor types, 40.0 mL of groundwater (B) or uranine-spiked groundwater to achieve the target concentration (WT, WTG) was added using calibrated pipettes or dispensers. The tubes

were sealed and put on an orbital shaker. The following procedure was strictly followed during sampling to minimize contamination or loss of samples. Reactors were incubated at target temperatures inside a thermocabinet throughout the experiment, as shown in Figure 4.



Figure 4 Reactors in a thermocabinet



Figure 5 Reactors after 24h in an orbital shaker

Each 50 mL reactor had to provide aliquots for fluorescence measurement, IC, and ICP analysis, and pH and EC determinations. Powder-free gloves were always worn, and new syringes and filters (0.45 µm pore size) were used for each sample. Syringes were pre-rinsed with the sample, and filters were conditioned by pulling a small volume of sample through the filter to reduce artifacts caused by adsorption to plastics and filter media.

The following sequence was applied at each sampling time:

- Centrifuge the reactors with gneiss.
- Allocate subsamples for:
  - fluorescence measurement;
  - IC-A (anion analysis, unacidified, stored cool);
  - IC-C (cation analysis, acidified with two drops of 6 % HNO_3);
  - ICPOES (metal analysis, unacidified, stored cool);
  - pH, EC and carbonate hardness determinations.

4.3 Analytical methods

4.3.1 Fluorescence spectroscopy

All samples containing gneiss were centrifuged prior to analysis using a Sorvall Lynx 6000 centrifuge (Thermo Fisher Scientific, USA) for 10 min at 3000 rpm to remove suspended solids and obtain clear supernatants for analysis (see Figure 6).



Figure 6 Reactors containing rock media are being centrifuged

Uranine concentrations were measured using a Cary Eclipse Fluorescence Spectrometer (Agilent Technologies, USA; serial number MY2519CG02). These fluorescence measurements were carried out by F. Schenker. The spectrometer was operated in emission scan mode with excitation at 491 nm and emission collected from 500–700 nm. Both excitation and emission slits were set to 5 nm; the scan rate was 600 nm min^{-1} with a data interval of 1 nm and an averaging time of 0.1 s. The photomultiplier tube (PMT) voltage was set to medium. Measurements were performed using a multicell holder with automatic excitation filtering and with the emission filter open. Acryl cuvettes of 1 cm path length were used for all measurements.

Fluorescence intensity at the emission maximum (~512 nm) was used as an analytical signal and is reported in arbitrary units (a.u.) As the fluorescence intensity of uranine is temperature dependent [14] and some matrix effects (ionic strength, pH, dissolved solutes) were observed, separate calibration curves were constructed for each experimental temperature using WT reactors without gneiss. After an equilibration time of 24 h, the WT reactors at 0.5, 5, 20, and 50 µg L^{-1} were analyzed. Samples were incubated at the target temperatures before analysis, but fluorescence was measured afterwards under identical laboratory conditions rather than directly at 10, 25, or 55 °C inside a temperature-controlled cuvette holder. Accordingly, the calibration curves are

specific to the equilibration temperature of the samples, not to real-time in-cuvette measurement temperature.

Initial and final concentrations in WT systems were considered equal because no solid phase was present and no significant retardation or loss mechanisms were expected over this time scale.

4.3.2 Ion chromatography and ICP-OES

Dissolved concentrations of the major anions (Cl^-, NO_3^-, SO_4^{2-}, Br^-) and major cations (Na^+, K^+, Mg^{2+}, Ca^{2+}) were determined by ion chromatography using an 881 Compact IC Pro for anion analysis and an 850 Compact IC Pro for cation analysis (Metrohm AG, Switzerland). These ion chromatographic analyses were carried out by Rebekka Wiedener. Multi-element standards containing known concentrations of fluoride, chloride, nitrite, bromide, nitrate, phosphate, and sulphate were used for instrument calibration, and method blank and quality-control standards were included in each analytical batch. Prepared samples ready for ion chromatography analysis are shown in Figure 7.

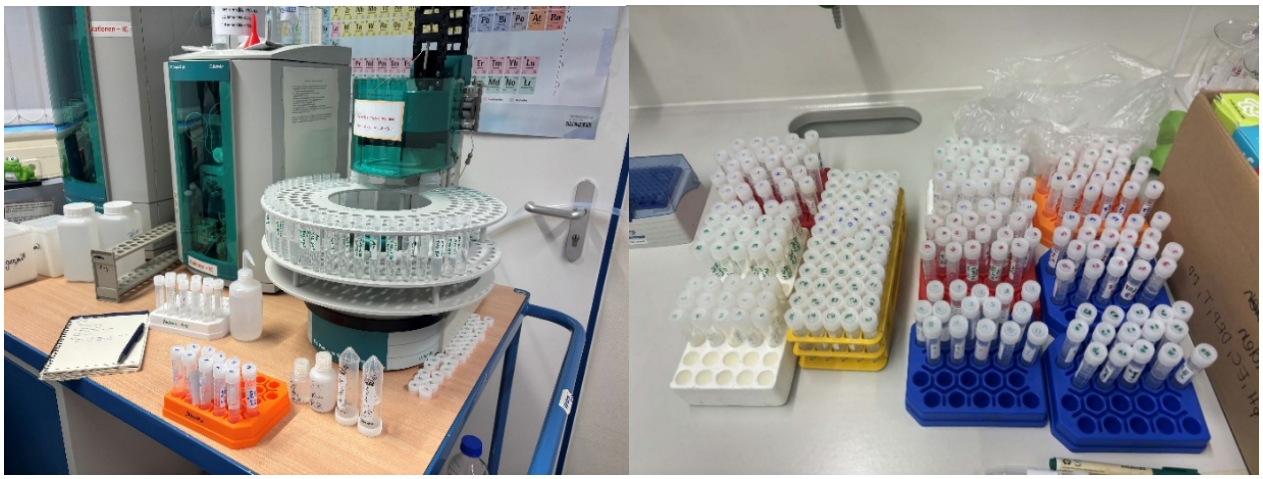


Figure 7 IC samples before testing

Selected trace metals (e.g. Fe, Mn, Al) were additionally analyzed by inductively coupled plasma optical emission spectrometry using an Agilent 5900 ICP-OES. These measurements were carried out by Dr Christine Viehweger and Rebekka Wiedener. Samples for ICP-OES were filtered and acidified shortly after collection with concentrated acid in order to stabilize dissolved metal concentrations and minimize precipitation or adsorption to container walls. Precision and accuracy were assessed using

multi-element external calibration standards, method blanks, and calibration-verification standards.

4.3.3 Field parameters and carbonate hardness

As shown in Figure 8, the pH, EC, and temperature measurements were performed using an HQ40d multimeter (Hach, USA) and the corresponding sensors (CDC401 conductivity sensor, Serial Number 240592583103). Carbonate hardness (acid neutralizing capacity, ANC) was determined titrimetrically using a MColortest™ kit (Merck, Germany) following acid neutralization to pH 4.3. It was measured to assess the buffering capacity of water, which is known to control pH, thus the fluorescence response. Carbonate hardness was determined by titration, as illustrated in Figure 9. Pipetting for preparation and handling of samples for all analyses was performed using calibrated Eppendorf Reference pipettes (Eppendorf SE, Germany; serial numbers 743280032, 3492935, 4042016; calibrated January 2026).

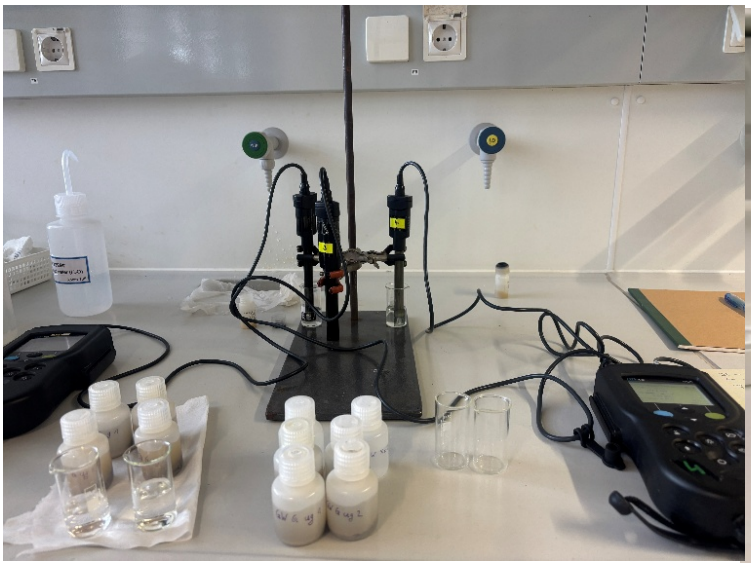


Figure 8 EC, pH, and temperature measurement using a multimeter



Figure 9 Titration process to test carbonate hardness

4.4 Data treatment

4.4.1 Calculation of ionic strength, hardness, and alkalinity

Ionic strength was calculated using equation (1):

$$I = \frac{1}{2}\sum c_i z_i^2 \quad (1)$$

Ionic strength, I (mol L^{-1}), calculated from molarity, c_i, and ionic charge, z_i, of each major ion in solution.

Total hardness (TH) was calculated as:

$$TH = 2.497[Ca^{2+}] + 4.118[Mg^{2+}] \quad (2)$$

Total hardness TH (mg L^{-1} as $CaCO_3$) calculated from Ca^{2+} and Mg^{2+} mass concentrations using standard stoichiometric factors.

4.4.2 Calculation of Release per Unit Mass

Element release was quantified by comparing the concentration of ion X in WT versus WTG reactors under identical experimental conditions (temperature and initial nominal uranine concentration). The difference attributable to the addition of gneiss for each ion is:

$$\Delta C_X = C_X(WTG) - C_X(WT) \quad (3)$$

Net change in dissolved ion concentration ΔC_X (mg L^{-1}) due to the gneiss addition, where positive values indicate net release and negative values indicate net uptake.

The total mass of X exchanged between rock and water in a 40 mL reactor is:

$$M_x = \Delta C_x \times 0.04 \quad (4)$$

Total mass $M_X(mg)$ of ion X exchanged between rock and water in a single 40 mL batch reactor.

Mass-normalized release (or uptake) per unit rock mass is:

$$R_x = \frac{M_x}{m_{gneiss}} = \frac{\Delta C_x \times 0.04}{13.3}$$

(5)

Mass-normalized release, R_X (mg g^{-1} or µg g^{-1}), of ion X per unit rock mass, equivalent to M_X divided by the gneiss mass (13.3 g) used in each WTG reactor.

4.4.3 Calculation of sorption

Intensity–concentration pairs were regressed for each temperature by ordinary least squares to obtain a linear calibration equation of the form:

$$I = a_r + b_r C$$

(6)

Linear fluorescence calibration relating fluorescence intensity, I (a.u.), to uranine concentration, C (µg L^{-1}), with temperature-specific intercept, a_r, and slope (sensitivity), b_r.

Uranine concentrations in WT and WTG samples were then calculated as:

$$C = \frac{I - a_r}{b_r}$$

(7)

Inverse calibration relationships are used to calculate uranine concentration C from measured fluorescence intensity, I, using the temperature-specific parameters a_r and b_r.

Matrix blanks (B) were measured at each temperature to quantify background fluorescence and to confirm a negligible native fluorescence signal from Freiberg groundwater.

Calculations followed standard batch equilibrium practice and OECD Guideline 106 [10], adapted to the uranine–gneiss system. For each temperature and initial concentration, the mean initial aqueous uranine concentration C_0 was taken from the corresponding WT reactors (matrix-matched calibration standards) at that temperature. This approach accounts for any small deviations from nominal concentrations due to stock preparation or dilution. The equilibrium concentration in each WTG reactor was obtained by converting the measured fluorescence intensity to concentration using the appropriate

temperature-specific calibration. The sorbed amount per unit mass of gneiss, q (µg/g), was calculated by mass balance:

$$\mathrm{q} = \frac{(\mathrm{C_0} - \mathrm{C_{eq}})\mathrm{V}}{\mathrm{m}} \tag{8}$$

Mass-balance expression for the sorbed amount, q (µg g^{-1}), onto gneiss, where C_0 is initial aqueous uranine concentration, C_{eq} is the equilibrium aqueous concentration, V is solution volume, and m is the mass of oven-dry gneiss.

The percentage of uranine removed from the solution was:

$$Sorption(\%) = \frac{(C_0 - C_{eq})}{C_0} \times 100 \tag{9}$$

Percentage of uranine removed from solution, calculated from the initial (C_0) and equilibrium (C_{eq}) aqueous concentrations.

and the apparent distribution coefficient K_d (L/kg) was calculated as:

$$K_d = \frac{q}{C_{eq}} \tag{10}$$

Apparent linear distribution coefficient, K_d (L kg^{-1}), defined as the sorbed amount, q, divided by the equilibrium aqueous concentration, C_{eq}.

These definitions are consistent with those used in other batch sorption studies on dyes and organic compounds.

4.4.4 Statistical analysis

All experiments were conducted in triplicate for each temperature–concentration combination, and treatment means, standard deviations, and standard errors were calculated for q, sorption percentage, and K_d. To evaluate whether observed sorption was distinguishable from zero within each treatment, a one-sample t-test was applied to the replicate q values against the null hypothesis $q = 0$. In parallel, a minimum detectable

sorbed amount was used as an analytical screening criterion, with $MDL_q = 0.003169$ in the same units as q. Cases in which the mean q exceeded MDL_q and the 95% confidence interval did not include zero were interpreted as significant sorption, whereas values below MDL_q or with confidence intervals spanning zero were classified as no detectable sorption.

To assess the combined effects of experimental factors, a two-factor ANOVA with replication was performed using q as the primary response variable. The fixed factors were initial uranine concentration at four levels (0.5, 5, 20, and 50 μg L^{-1}) and temperature at three levels (10, 25, and 55 °C), with three replicate WTG reactors per treatment combination. The ANOVA tested the main effects of concentration and temperature, as well as the concentration × temperature interaction, with statistical significance assessed at $\alpha = 0.05$. Statistical calculations were carried out in Microsoft Excel using the Data Analysis ToolPak.

For every combination of temperature and concentration, we performed three replicates, then calculated the means, standard deviations (SDs), and standard errors of the mean (SEMs) for q, sorption percentage, and K_d. For each treatment, sorption different from zero was determined by performing a one-sample t-test of the three replicate q values against a theoretical mean of $q = 0$. A minimum detectable sorbed concentration $MDL_q = 0.003169$ in units of q, was also used as a screening tool in the analysis. If both the mean q exceeded MDL_q and its 95% confidence interval did not contain zero, then the observations were considered as evidence for sorption; observations with mean q below MDL_q or with a confidence interval that contained zero were considered as evidence for zero sorption. A two-factor replicated analysis of variance (ANOVA) was conducted using q as the response variable to determine the joint significance of experimental factors. Fixed factors included initial uranine concentration with four levels (0.5, 5, 20, and 50 μg L^{-1}) and temperature with three levels (10, 25, and 55 °C), and there were three replicate WTG reactors for each treatment combination. ANOVA was used to test the significance of concentration and temperature main effects, as well as the concentration and temperature interaction using $\alpha = 0.05$. Statistical analysis was performed in Microsoft Excel using the Data Analysis ToolPak.

5. Results

The experimental data are reported systematically, moving from water chemistry through element release to uranine fluorescence and sorption outcomes.

5.1 Hydrochemical Characterization

5.1.1 Long-term Field Monitoring and Baseline Groundwater Chemistry

Routine monitoring at the Freiberg test site between 2020 and 2025 indicates that the groundwater is moderately mineralized and chemically stable over multi-year timescales. Historical groundwater chemistry data used for comparison were provided by F. Schenker as unpublished monitoring data (personal communication, 2025). The major-ion composition of the Freiberg groundwater is summarized in Table 1. Anions in 2020–2022 were dominated by chloride (Cl^-: 144–260 mg L^{-1}), sulphate (SO_4^{2-}: 125–133 mg L^{-1}), and nitrate (NO_3^-: 19–24 mg L^{-1}), with bromide (Br^-: 0.2–0.6 mg L^{-1}) and fluoride, nitrite, and phosphate mostly below 0.1 mg L^{-1}. Major cations included sodium (Na^+: 38–60 mg L^{-1}), potassium (K^+: 5.0–6.1 mg L^{-1}), magnesium (Mg^{2+}: 22–31 mg L^{-1}), and calcium (Ca^{2+}: 86–114 mg L^{-1}).

Table 1 Major-ion composition of groundwater from the Freiberg gneiss aquifer.

Parameter (mg/l)	Year				
	2021	**2022**	**2023**	**2024**	**2025**
Chloride	144.03	260	206.3	157.92	194
Nitrate	19.26	22	21.1	16.73	-
Sulphate	125.2	133	116.98	95.4	105
Sodium	37.97	52	60.26	44.517	54
Potassium	5.33	5.7	6.14	4.685	5.02
Magnesium	22.41	30	31.46	23.158	24.3
Calcium	85.81	114	-	114.363	83.4

Long-term field parameters are reported in Table 2. Total hardness was consistently high (18–20 °d; ca. 320–360 mg L^{-1} as $CaCO_3$), while carbonate hardness declined from 7 °d (2020) to 5.5 °d (2021) and further to 1.5–1.6 °d by 2024. Electrical conductivity ranged

from 851 to 1052 µS cm^{-1}, and pH remained slightly acidic to near-neutral (5.3–6.0), with stable groundwater temperatures around 11.5–12.3 °C.

Table 2 Field parameters of groundwater from the Freiberg gneiss aquifer.

Parameter	Unit	Year				
		2020	2021	2022	2023	2025
Total hardness	°d	-	18	17.8	20.2	15.8
Total hardness	mg L^{-1} as $CaCO_3$	-	320	-	360	270
Carbonate hardness	°d	-	7	5.5	1.55	1.2
SEC	µS cm^{-1}	883	851	900	930	1052
pH	-	6.03	5.3	5.6	5.56	5.63
Dissolved oxygen	mg L^{-1}	5.24	4.95	5	5.24	4.91
Water temperature	℃	11.5	11.6	11.6	-	12.3
Turbidity	FNU	9.43	-	-	-	-

The laboratory sample OG 1, designated hereafter as “original” experimental water, replicates that field composition. Ion chromatography and ICP-OES (see Table 3) analysis of OG 1 gave Na^+ = 58.6 mg L^{-1}; K^+ = 5.36 mg L^{-1}; Mg^{2+} = 26.85 mg L^{-1}; Ca^{2+} = 91.26 mg L^{-1}; Br^- = 0.34 mg L^{-1}; NO_3^- = 19 mg L^{-1}; Cl^- = 215.6 mg L^{-1}; and SO42− = 108.5 mg L−1. Addition of the major ions gives a total dissolved solids (TDS) concentration of ~515–525 mg L−1 (not including bicarbonate), which agrees well with the conductivity measurement and field hardness.

5.1.2 Ionic strength, hardness, alkalinity

Applying equation 1 to OG 1, converting mass concentrations to mol L^{-1} using standard molar masses gives monovalent and divalent contributions of, respectively, which together give an ionic strength of order 10 $^{-2}$ M typical of moderately mineralized Ca–Na–Cl–SO_4 groundwater. Table 3 lists measured cation and anion concentrations of the experimental waters.

Applying equation 2 to OG 1, Ca^{2+} = 91.26 mg L^{-1} and Mg^{2+} = 26.85 mg L^{-1} gives TH ≈ 338 mg L^{-1} as $CaCO_3$ (≈ 18.9 °d), very close to field hardnesses of ~18 °d. Carbonate hardness (CH) field values from titrations were 7 °d in 2020 and 5.5 °d in 2021 (≈125 and 98 mg L^{-1} as $CaCO_3$), suggesting that ~ one-third of total hardness is associated with carbonate and ~ two-thirds is non-carbonate (associated with Cl^- and SO_4^{2-}). This

suggests that carbonate minerals are not the sole source of Ca^{2+}–Mg^{2+}, and that silicate weathering and sulphate/chloride sources are additionally important.

Table 3 Measured cation and anion concentrations (mg L^{-1})

Temp.	n	Na^+	K^+	Mg^{2+}	Ca^{2+}	Br^-	NO_3^-	Cl^-	SO_4^{2-}
Original	1	58.58	5.36	26.85	91.26	0.34	19.00	215.6	108.5
	2	58.31	5.44	26.87	91.40	0.34	18.62	212.9	107.5
	3	58.79	5.41	26.86	91.37	0.34	18.62	215.3	108.9
55 °C	1	57.96	5.45	27.17	92.63	0.34	18.90	210.5	106.2
	2	57.86	5.33	27.09	92.18	0.34	18.25	213.0	107.8
	3	58.72	5.40	27.09	92.04	0.34	18.77	210.7	106.3
20 °C	1	57.94	5.42	26.98	91.76	0.35	17.63	214.3	107.2
	2	58.06	5.37	27.01	91.90	0.35	18.75	214.4	108.1
	3	58.46	5.39	26.93	91.65	0.35	18.03	212.3	107.7
10 °C	1	57.01	5.54	26.70	90.82	0.38	18.46	211.1	105.9
	2	56.88	5.35	26.52	90.25	0.38	18.43	211.8	106.0
	3	57.21	5.31	26.47	90.11	0.38	18.54	211.5	106.2

5.1.3 Experimental Waters and Charge Balance

“Original” groundwater and the concentrated/diluted blanks had internally consistent major-ion compositions, with variations around OG 1 values only being minor. Sodium concentrations varied around 57–59 mg L^{-1}, potassium around 5.3–5.4 mg L^{-1}, magnesium 25–27 mg L^{-1} and calcium 90–93 mg L^{-1} among the blanks. Chloride concentrations were consistently around 210–228 mg L^{-1} and sulphate around 108 mg L^{-1} from repeated analyses of the blank waters. Nitrate and bromide remained low in all samples. Table 4 shows the charge balance of all blank waters. The charge-balance errors (CBE %) fell within ±5 % and varied from cation sums of 9.30–9.52 meq L^{-1} and anion sums of 8.46–8.65 meq L^{-1}, giving an average CBE ≈ 5 %. The systematic excess of cations of ≈5 % is attributed to unmeasured bicarbonate and suggests the IC/ICP-OES data are accurate enough to discuss small changes in concentration induced by water–rock interaction.

Table 4 Cation and anion charge-balance

Sample	n	Σ cations (meq/L)	Σ anions (meq/L)	CBE (%)	Interpretation
Baseline groundwater	3	9.4532	8.6151	4.64	Acceptable charge balance
Groundwater equilibrated at 55 °C	3	9.5045	8.4911	5.63	Near threshold; small cation excess
Groundwater equilibrated at 20 °C	3	9.4659	8.5658	4.99	Acceptable charge balance
Groundwater equilibrated at 10 °C	3	9.3149	8.4756	4.72	Acceptable charge balance

5.1.4 Field Parameters in WT and WTG Reactors

Batch experiments used three system types at each temperature and nominal uranine concentration: Blank (groundwater only), WT (water and tracer) and WTG (water, tracer and gneiss). Field measurements of carbonate hardness, pH, temperature, and electrical conductivity (EC) were made in WT and WTG reactors after 24 h.

Carbonate hardness in all reactors was low (≈ 1.4–3.0 °d), and similar between WT and WTG; small WTG–WT differences were within measurement resolution. pH remained near neutral to slightly alkaline (ca. 6.3–7.2) in all treatments, with paired differences typically ≤ 0.2 units, indicating no systematic acidification or alkalization due to gneiss addition. Measurement temperatures were between 17.4 and 20.9 °C for both series, with closely matched WT–WTG pairs.

By contrast, electrical conductivity showed a clear systematic difference: WTG EC values were consistently higher than WT by tens to > 200 µS cm^{-1}. Most measurements fell around 1030–1143 µS cm^{-1}, with a maximum of 1310.3 µS cm^{-1} in WTG at the highest nominal concentration, compared to 1073.3 µS cm^{-1} in the corresponding WT. This pattern indicates slight but reproducible increases in mineralization due to water-rock interaction with the gneiss, while pH and carbonate hardness remained effectively unchanged (detailed table in Appendix B.1.) Electrical conductivity across all temperature and concentration conditions in WT and WTG reactors is presented in Figure 10.

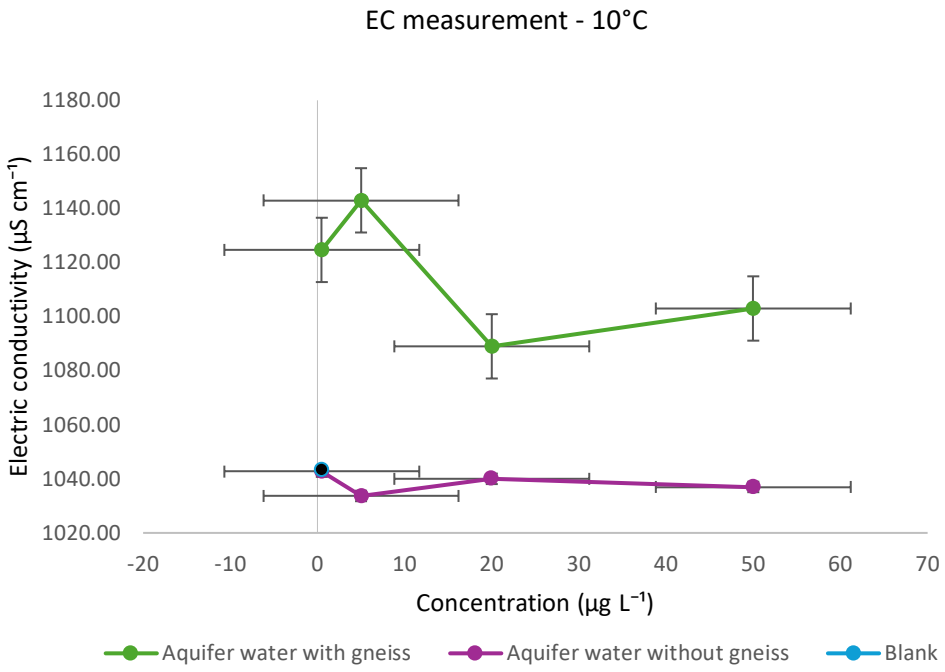


Figure 10 Electrical conductivity in WT and WTG reactors at all tested temperatures and nominal uranine concentrations.

5.2 Element Release from Gneiss in Batch Reactors

5.2.1 Major-Ion Behavior in WT and WTG Systems

The major cation contents of the starting waters were almost unaffected by temperature and uranine concentration (see Figure 11). In this regard, we can assume that the background groundwater chemical composition did not change independently of gneiss addition by changing either temperature or uranine concentration. The control water therefore can be considered chemically stable throughout the experiment and changes within the reactors containing gneiss occurred primarily due to water-rock interaction.

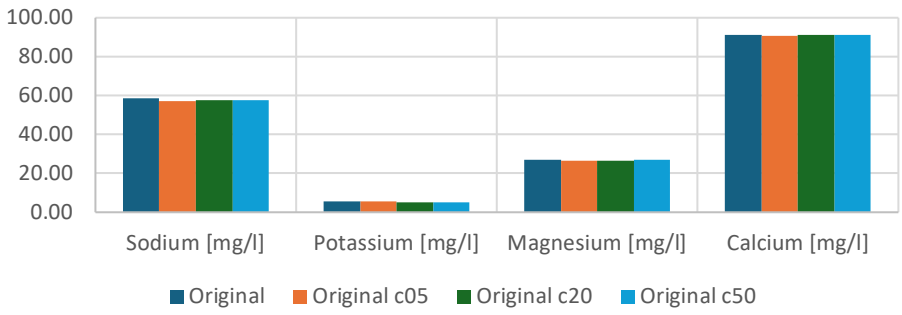


Figure 11 Major cation concentrations in the original groundwater and its temperature treatment variants without gneiss.

Ion chromatography analyses of Blank, WT, and WTG reactors show that in WT reactors (no gneiss), cation and anion concentrations remain essentially equal to the Blank values, confirming that uranine addition and incubation do not alter major-ion chemistry within analytical uncertainty. In WTG reactors, however, systematic increases in several ions were observed. The ion release attributable to gneiss was calculated as the difference between WTG and WT concentrations, as given in equation (3).

Across all temperatures and uranine concentrations, WTG reactors show typical average increases (relative to WT) of approximately:

- Na^+: +5 mg L^{-1}
- K^+: +7 mg L^{-1}
- Mg^{2+}: +1.3 mg L^{-1}
- Ca^{2+}: +7.3 mg L^{-1}
- Cl^-: +5–13 mg L^{-1}
- SO_4^{2-}: +12–20 mg L^{-1}

For the 40 mL reactor volume and 13.3 g gneiss, these correspond to mass-normalized releases of order (using equation 5):

- Na^+: ~15 µg g^{-1}
- K^+: ~21 µg g^{-1}
- Mg^{2+}: ~4 µg g^{-1}
- Ca^{2+}: ~22 µg g^{-1}

Chloride increases of 5–13 mg L^{-1} equate to ca. 15–40 µg g^{-1}, and sulphate increases of 12–20 mg L^{-1} to about 36–60 µg g^{-1}. These values illustrate that the gneiss acts as a weak but consistent source of Na^+, K^+, Mg^{2+}, Ca^{2+}, Cl^- , and SO_4^{2-} over 24 h (detailed measurement values are in Appendix A). Charge-balance calculations for WT and WTG samples confirm that these changes are analytically robust: CBE% remains within ±5% and shows a similar small cation excess as in OG 1, implying that released anions are largely accounted for.

5.3 Fluorescence Calibration and Temperature Dependence of Uranine

5.3.1 Temperature-Specific Calibration Curves

The resulting temperature-specific calibration curves,for uranine at 10 °C, 25 °C, and 55 °C are presented in Figure 12. Fluorescence intensity was related to concentration by the linear equation (6). The concentration of uranine in each sample was then back-calculated using equation (7).

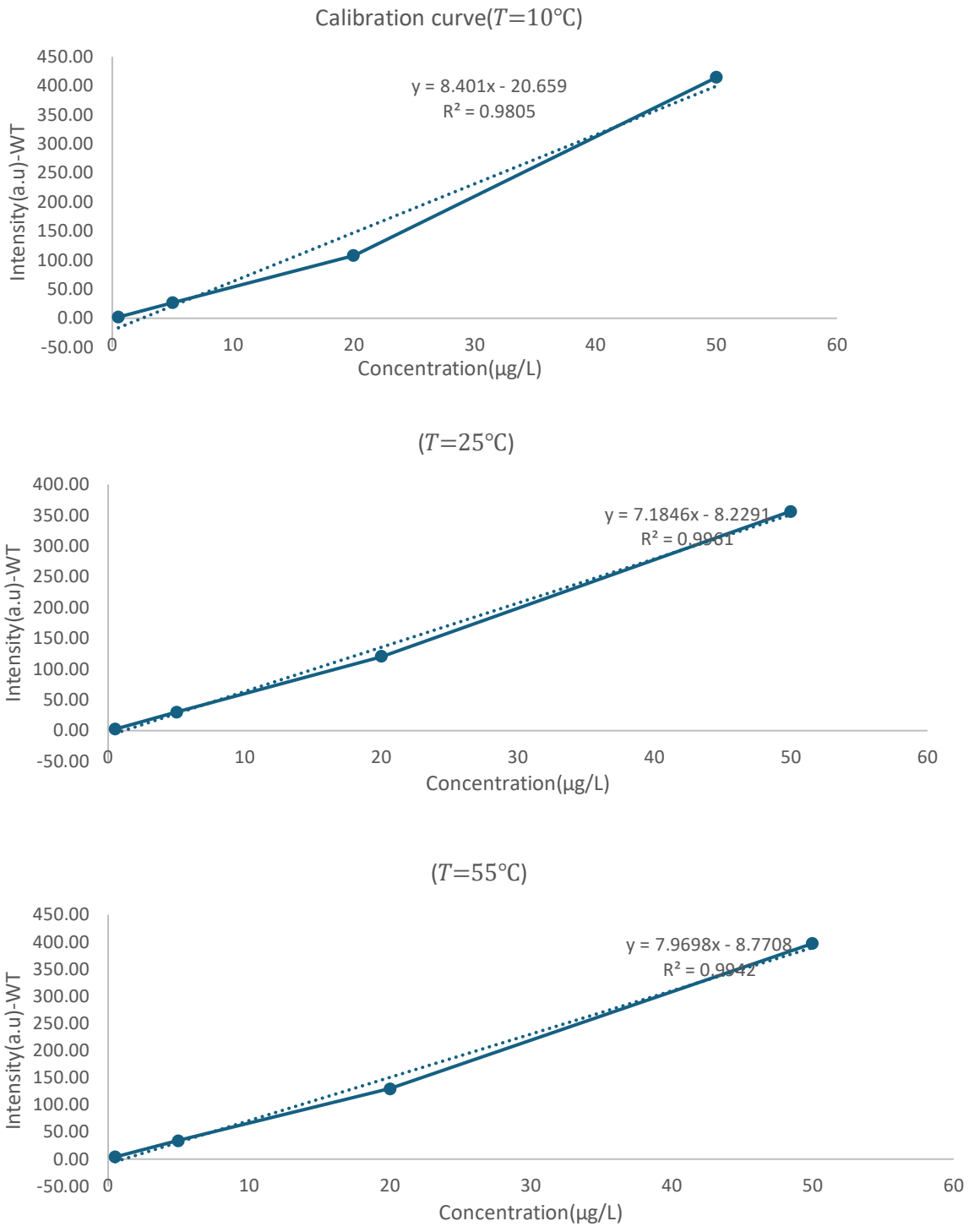


Figure 12 Temperature-specific calibration curves for uranine fluorescence at 10 °C, 25 °C, and 55 °C.

Using matrix-matched and temperature-specific calibration curves implicitly correct for thermal quenching and groundwater matrix effects on fluorescence, removing the need for separate empirical temperature correction factors in the subsequent concentration calculations (values used to plot the curve are shown in Appendix B.1).

5.4 Uranine Sorption onto Gneiss

5.4.1 Sorbed Amounts and Distribution Coefficients

Mean sorbed amounts and 95% confidence intervals for all treatment combinations are given in Table 5. The mass of uranine sorbed per unit mass of gneiss, q, was calculated according to equation (4). At the two lowest nominal uranine concentrations (0.5 and 5 µg L^{-1}), calculated q-values are low in magnitude (often slightly negative or near zero), and never exceed MDL_q. For instance, at 10 °C and 0.5 µg L^{-1}, individual q values range from about −0.0016 to −0.0027 (µg g^{-1}) with small standard deviations, and mean q is lower than MDL_q. The corresponding t-statistics are $|t| < 4.3$, so the null hypothesis that sorption is zero cannot be rejected. Results at 5 µg L^{-1} are similar (q-values near zero with overlapping confidence intervals).

At higher concentrations (20 and 50 µg L^{-1}), q values are clearly positive and exceed MDL_q under many conditions. For instance, at 10 °C and 20 µg L^{-1}, q values are of order 0.010–0.012 µg g^{-1}, corresponding to measurable removal from solution, while at 50 µg L^{-1} they increase to ~0.085–0.093. Calculated K_d values at 20 µg L^{-1} are small but positive; at 50 µg L^{-1} they are somewhat higher, reflecting greater sorbed mass at higher aqueous concentration.

Sorption percentages derived from C_0 and C_{eq} show the same pattern: at 0.5 and 5 µg L^{-1}, sorption (%) is near zero and within experimental uncertainty, whereas at 20 µg L^{-1} a few per cent of uranine are removed from solution, and at 50 µg L^{-1}, sorption (%) can reach several tens of per cent in some replicate sets.

Table 5 Mean uranine sorption (q, $\mu g\ g^{-1}$)

Temperature (°C)	Concentration (µg L^{-1})	Mean q (µg g^{-1})	95 % CI	Interpretation
10	0.5	−0.0020	−0.0035 to −0.0005	No detectable sorption
	5	−0.0012	−0.0176 to 0.0153	No detectable sorption
	20	0.0117	0.0079 to 0.0154	Detectable sorption
	50	0.0895	0.0787 to 0.1003	Strongest sorption
25	0.5	−0.0066	−0.0279 to 0.0148	No detectable sorption
	5	−0.0002	−0.0017 to 0.0013	No detectable sorption
	20	0.0048	0.0010 to 0.0086	Detectable sorption
	50	0.0115	0.0034 to 0.0195	Detectable sorption
55	0.5	−0.0001	−0.0004 to 0.0002	No detectable sorption
	5	−0.0015	−0.0185 to 0.0155	No detectable sorption
	20	0.0103	0.0061 to 0.0145	Detectable sorption
	50	0.0417	0.0269 to 0.0565	Detectable sorption

5.4.2 Statistical Evaluation and Minimum Detectable Sorption

The combined use of MDL_q and a conservative t-critical value (4.3) provides a transparent framework to differentiate true sorption from analytical noise. Cases where mean q exceeds MDL_q and the 95 % confidence interval does not include zero are interpreted as significant sorption; those where q is below MDL_q or confidence intervals that span zero are classed as no detectable sorption.

5.4.3 Factorial effects of concentration and temperature on uranine sorption

ANOVA table 6 presents the two-factor ANOVA results. Two-factor ANOVA revealed highly significant effects of concentration (SS = 0.014918, df = 3, F = 250.27, p = 3.1 × 10−18), temperature (SS = 0.002948, df = 2, F = 74.17, p = 5.32 × 10−11), and interaction (SS = 0.006498, df = 6, F = 54.50, p = 8.34 × 10−13) on q. Concentration was the largest source of variation among the fixed factors examined, whereas significant interaction suggests concentration-dependent response to temperature. Inspection of the treatment

means revealed that q values remained near zero at 0.5 and 5 µg L−1 but became positive at 20 and 50 µg L−1 suggesting that sorption was detectable only above the low-concentration range.

Table 6 Two-factor ANOVA table for uranine sorption (q) with concentration, temperature, and their interaction as fixed factors.

Source of Variation	SS	df	MS	F	p-value	F crit
Concentration	0.014918	3	0.004973	250.27	3.1×10^{-18}	3.009
Temperature	0.002948	2	0.001474	74.17	5.32×10^{-11}	3.403
Interaction	0.006498	6	0.001083	54.50	8.34×10^{-13}	2.508
Within	0.000477	24	1.99×10^{-5}	—	—	—

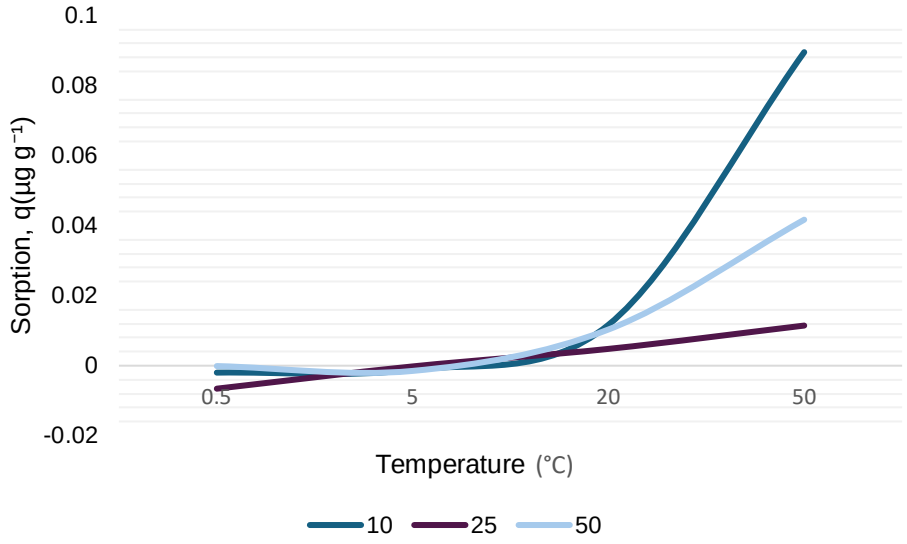


Figure 13 Sorption versus nominal uranine concentration, with separate curves for 10 °C, 25 °C, and 55 °C

This pattern is illustrated in Figure 13, in which the curves for 10, 25, and 55 °C are not fully parallel, confirming that the concentration response of uranine sorption changes with temperature.

At low concentrations, mean sorption values were negative or near zero and remained below the detection-oriented decision threshold, whereas at 20 and especially 50 µg L^{-1}, sorption became consistently positive.

Taken together, the ANOVA and interaction plot show that concentration was the dominant control on *q*, while temperature modified this response in a non-monotonic manner.

5.5 Integrated Assessment of Uranine Behavior and Element Release

Combining hydrochemical characterization, major-ion release, and uranine sorption leads to the following integrated picture:

The experimental groundwater is a moderately mineralized Ca–Na–Cl–SO_4 water with high hardness and slightly acidic to near-neutral pH, closely reflecting the long-term field composition of the fractured gneiss aquifer.

Addition of 13.3 g gneiss to 40 mL groundwater for 24 h produces small but systematic increases in Na^+, K^+, Mg^{2+}, Ca^{2+}, Cl^- and SO_4^{2-}, corresponding to mass-normalized releases of order 4–60 µg g^{-1}, while pH and carbonate hardness remain unchanged. This confirms mild but detectable water–rock interaction under the experimental conditions.

Uranine fluorescence in this groundwater shows a strong, approximately linear relationship with concentration at each temperature, but also pronounced thermal quenching that must be accounted for by temperature-specific calibration.

After calibration, uranine sorption onto gneiss is not detectable at low concentrations (≤ 5 µg L^{-1}) within the detection limits of the experiment but becomes weakly positive at 20 µg L^{-1} and more pronounced at 50 µg L^{-1}, with modest temperature dependence.

Taken together, these results indicate that in the Freiberg fractured gneiss aquifer, and under the chemical conditions studied, uranine is effectively conservative at the low concentrations typical of many field tracer tests, yet it can experience measurable retention at elevated concentrations and over longer timescales, particularly when combined with matrix diffusion and water–rock interaction. This has direct implications for the design and interpretation of uranine tracer experiments in crystalline aquifers.

6. Discussion

The results are critically evaluated against published evidence and translated into practical guidance for hydrogeological tracer applications.

6.1 Interpretation of Release Patterns

The observed increases in Na^+, K^+, Mg^{2+}, and Ca^{2+} are consistent with early stage water rock interaction and dissolution of silicate minerals in the gneiss, which is a recognised control on groundwater chemistry in crystalline and gneissic terrains [18,19]. The accompanying increase in SO_4^{2-} can plausibly reflect oxidation of trace sulphide minerals such as pyrite under oxic batch conditions, which is a well-documented source of dissolved sulphate in groundwater systems [20, 21]. By contrast, the increase in Cl^- should be interpreted more cautiously, because chloride may derive from multiple natural or external sources and cannot be assigned confidently to a specific mineral source without additional mineralogical evidence [23]. Since the experiments were conducted as short term batch tests with crushed rock, the measured ion release is best interpreted as an accelerated laboratory response rather than a direct representation of in situ fracture wall weathering, because laboratory and field weathering rates commonly differ where reactive surface area, particle size distribution, temperature, and heterogeneity are not comparable [22].

Despite measurable release of cations and anions, pH and carbonate hardness remain unchanged, indicating that carbonate equilibria and buffering are only weakly perturbed in these short-term batch experiments.

Because the specific surface area of the gneiss is not yet known, conversion of these mass-normalized releases to area-normalized weathering rates (mol m^{-2} s^{-1}) is not attempted. Instead, R_X values are used as a comparative metric of reactivity between ions, temperatures, and experimental conditions, with a clear route outlined for later conversion once BET data become available.

6.2 Temperature effects on fluorescence versus sorption

Temperature exerted a strong control on uranine detectability but only a secondary control on uranine sorption in these experiments. Fluorescence was strongly correlated to

concentration approximately linearly at each temperature measured in this study, but the raw signal was significantly dampened by thermal quenching, which necessitates temperature-specific calibration before interpretation of any potential sorption. This finding is consistent with Blaen et al., who observed strong negative temperature effects on fluorescent signal intensity, stronger impacts at low concentrations, and considerable uncertainty in tracer breakthrough curves where both turbidity and temperature were not accounted for.

Importantly, these three temperature levels are not of equivalent environmental significance and should be interpreted distinctly. The 10 °C treatment approximates Freiberg site conditions most closely (near groundwater temperatures of 12 °C were recorded at the study site), whereas 25 °C represents a relevant temperate and laboratory control condition. The third treatment temperature of 55 °C was not intended to represent groundwater conditions at the Freiberg site. Rather, it serves as an upper-bound test of uranine behaviour under significantly elevated temperature conditions. This condition allows for interpretation beyond the Freiberg site by providing insight into potential temperature dependencies of thermal quenching and sorption in deeper, warmer, or otherwise thermally fractured aquifer systems with groundwater temperatures exceeding those found in shallow, temperate environments. Therefore, the results of the 55 °C treatment should be regarded as a bounding condition from which potential transferability of data may be derived.

The alignment between these data and Blaen et al.'s results is critical because it validates the primary methodological approach of this work. Prior research has demonstrated that phenomena that appear as tracer loss may be changes in fluorescence response, and this dataset confirms that such changes can obscure the interpretation of recovery in fractured-rock tracer studies where transport is presumed to be the only influencing factor (5). Temperature's primary impact on recovery after calibration was through measurement sensitivity rather than actual sorption mass balance, which was visible once again after sorption onto gneiss did not appear at 0.5 and 5 µg/L but turned weakly positive at 20 µg/L and substantially positive at 50 µg/L.

6.3 Comparison with the wider tracer literature

That observed sorption behavior agrees with expectations based on the wider tracer bibliography as well. Bork et al. showed that uranine retention depends on the geological

matrix, growing strongest at lower pH values but also with increasing clay content and increasing organic carbon, such that adsorption can approach complete removal in clay-amended systems yet stay relatively low in sandy substrates near neutral pH [6]. In classic tracer reviews, authors reported qualitatively similar findings: uranine behaves most conservatively in low-organic, low-clay content materials and can be progressively sorbed under acidic, clayey, or humic conditions [8]. Given those results, low uranine sorption on Freiberg gneiss at concentrations near 5 µg/L is reasonable because pH remained near neutral with little variation during batch tests and water-rock interaction was limited but measurable.

Conversely, the data set argues against calling uranine universally conservative in fractured gneiss environments. While tracer loss was not observed at low concentrations within the limits of detection, uranine retention became quantifiable at 20 µg/L and increased again at 50 µg/L, showing that concentration can exert a stronger control than temperature where both are varied. Sabatini and colleagues observed parallel results for consolidated aquifer materials, reporting low but non-zero sorption for anionic dyes like fluorescein in sandstone-like media and explaining how even in cases where equilibrium sorption is weak, intraparticle diffusion may still cause transport tailing [4]. Thus, uranine should likely be considered conditionally rather than strictly conservative in crystalline aquifers.

6.4 Implications for field tracer tests

That consideration is especially relevant to field studies. Conservative salts were used in previous tracer experiments at the Freiberg site, and researchers ascribed late-time breakthrough tailing to dual-porosity exchange, immobile porosity, and fracture-matrix diffusion. This new result does not necessarily conflict with those hydraulic interpretations of retardation, but it suggests that tracer tests using fluorescent dye may incorporate a chemical-retention component at higher uranine concentrations. Conceptually, this amounts to the recommendation that tracer tests in fractured crystalline rock cannot always assume highly long-tailed breakthrough curves to be solely the result of matrix diffusion or immobile porosity if a reactive fluorescent dye is applied.

Crucially, however, these batch results do not indicate breakthrough tailing directly. They point to a credible chemically based retention mechanism that, when added to physical mechanisms (matrix diffusion, immobile porosity, water-rock interaction etc.)

encountered in tracer tests in the field, could result in incomplete recovery or long-time tails. Conceptually, this means that late-time behavior observed in fluorescent dye tracer tests should not necessarily be ascribed to transport heterogeneity alone, especially if uranine concentrations are relatively high or residence times longer.

Literature on matrix effects helps to bolster this hypothesis. Weidner et al. found uranine detection to be influenced by low pH, dissolved Fe and Mn, mineral precipitation during the addition of a buffer, and spectral overlap from eosine, leading them to conclude that fluorometric tracer recovery is sensitive to both water chemistry and method of spectral analysis [3]. The groundwater at Freiberg is not acidic mine water and therefore does not replicate those findings exactly, but the principle that matrix interferences can impact fluorometric recovery holds true and supports the idea that site-specific calibration within the true groundwater matrix is needed to distinguish fluorescence loss from sorption-related mass loss with confidence.

6.5 Interpretation of concentration and temperature effects on sorption

Factorial analysis confirms the conclusion that uranine sorption on Freiberg gneiss is concentration-controlled rather than temperature-dependent. Sorption is insignificant within measurement uncertainty at 0.5 and 5 µg L^{-1}, turns positive at 20 µg L^{-1}, and increases in magnitude again at 50 µg L^{-1}.

This significant interaction tells us that temperature cannot be said to have one simple effect over the entire range of concentrations studied. Instead, temperature differences are minimal where sorption is zero or negligible but become pronounced when measurable sorption begins to occur at higher concentrations. Temperature effects were also non-monotonic, which suggests that temperature had a secondary effect compared to concentration under our batch testing conditions.

It also helps us to differentiate real sorption from fluorescence artefacts. Since concentrations were calculated from temperature-specific calibration curves, the differences seen in q represent differences in the mass balance after correction for thermal quenching rather than the direct effects of temperature on fluorescence intensity. The ANOVA therefore reinforces the interpretation that low concentration treatments were

effectively conservative, while higher concentrations exhibited weak but hydrologically significant retention.

Taken together, these results suggest that uranine can be considered effectively conservative in the Freiberg gneiss system at low concentrations common to many field tracer tests, but that concentration-dependent sorption must be considered when high tracer masses are applied or when interpreting breakthrough tailing in detail. Both sorption and temperature-corrected fluorescence response must be considered in such cases to prevent biased recoveries. However, these conclusions must be understood in the context of the batch experimental design employed in this study. Rather than testing intact fracture-wall surfaces under flowing conditions, experiments were conducted on dried, sieved, and mechanically altered gneiss, so the available reactive surface area was likely greater than would be present in situ in the subsurface. Furthermore, although the 24 h contact time was chosen to represent an approximate equilibrium period according to batch study protocols, previous studies on consolidated media have shown that sorption and intraparticle diffusion can continue past the 24 h mark for crushed rock samples and that intact-rock flow systems can more accurately represent field conditions. The processes of advective transport, fracture geometry, and fracture-matrix exchange cannot be directly simulated with batch reactors either. Therefore, the results presented here should be seen as limiting the extent to which sorption could contribute to uranine loss under these prescribed conditions, rather than completely describing in situ tracer transport through the Freiberg fractured gneiss aquifer.

6.6 Uncertainty and analytical limitations

The sorption results should be interpreted considering several analytical and methodological uncertainties. OECD Guideline 106 identifies analytical accuracy, attainment of equilibrium, soil-to-solution ratio, and structural changes in the sorbent during equilibration as key factors affecting the repeatability of sorption estimates [10]. In the present study, uncertainty arose primarily from the temperature-specific fluorescence calibration, replicate variability at each temperature and concentration level, and the propagation of small concentration differences through the mass-balance calculation used to derive sorbed mass, sorption percentage, and distribution coefficients.

Another analytical limitation to consider is the possible effect of turbidity on the fluorescence signal. Sample supernatants were treated to achieve complete clarity prior

to measurement, but residual sub-microscale particles might still have contributed to quenching of uranine fluorescence, as turbidity both shifts measured fluorescence intensity in an intensity-dependent way and warps the uranine spectral curve itself. This caveat is of special importance to the dataset presented here, because sorption was undetectable at 0.5 and 5 μg L^{-1}, weakly positive at 20 μg L^{-1}, and positively elevated only at 50 μg L^{-1}. Thus, any distortion of the signal caused by turbidity will have been greatest at low concentrations, where minor differences between WT and WTG fluorescence intensities were used to calculate sorbed mass and determine if a result was non-detectable or weakly positive.

Additional uncertainty may have been introduced during sample handling and filtration, although pre-rinsing of syringes and conditioning of filters were carried out to minimize possible adsorption artefacts on plastics and filter media. The relatively small number of replicates per treatment also limited statistical power, meaning that low-magnitude sorption effects, particularly at the lower concentration range, should be interpreted with caution.

Further limitation relates to the experimental design itself. The batch experiments were conducted using dried, sieved, and mechanically altered gneiss over a 24 h reaction period rather than intact fracture-wall surfaces under flowing conditions. As a result, the available reactive surface area was likely greater than that present in the subsurface, and the system may not fully reproduce in situ water-rock interaction in fractured gneiss aquifers. Previous work on consolidated media has also shown that crushed-rock systems may not reach equilibrium within 24 h and may overestimate sorption relative to intact rock surfaces.

A final methodological limitation is that agitation was not uniform between all batch runs, due to the mechanical irregularity of the shaker. This is relevant because equilibrium batch sorption experiments require sufficient agitation both to suspend the solid phase and ensure reproducible solution-to-substrate contact throughout equilibration. Irregular shaking during the experiments reported here could have impacted mass transfer between uranine and gneiss surfaces, equilibration within 24 h, and reproducibility between replicates. This caveat is also most applicable to the low-concentration, borderline range of the dataset, since concentrations of 0.5 and 5 μg L^{-1} yielded no detectable sorption and 20 μg L^{-1} yielded only weakly positive sorption. Minor differences in agitation could feasibly impact the calculated magnitude of uranine retention.

Accordingly, the data presented here should be regarded as a controlled laboratory estimate of relative uranine retention under the tested conditions rather than as a direct quantitative prediction of field-scale transport behaviour in the Freiberg fractured gneiss aquifer.

6.7 Contribution to literature

The motivation presented in Chapter 3 reveals a gap in the literature regarding fluorescent tracer studies conducted in crystalline rock matrices. Uranine sorption studies have been completed in many soil, sediment, sandstone, and limestone matrices as well as various model sorbents, but experimental data on sorption in gneiss and other crystalline rocks are limited, especially considering crystalline rocks host a significant portion of the world's groundwater supply and complicate tracer interpretation efforts. Specifically, batch sorption coefficients specific to the site of interest and fluorescence intensity-temperature relationships were unavailable prior to this research.

The secondary contribution of this work is technical in nature. While many uranine sorption experiments [15] were conducted at ambient temperatures (roughly 20-25 °C), fluorescence intensity and uranine sorption as functions of temperature have not been well documented in crystalline rock matrices. Generating matrix-matched fluorescence intensity calibration curves at specific temperatures allowed this thesis to differentiate between apparent tracer loss due to thermal quenching and true tracer retention as a result of absorption.

These findings add to the empirical dataset describing uranine behaviour in Freiberg fractured gneiss groundwater. Uranine fluorescence intensity was linearly proportional to concentration at each temperature sampled but exhibited significant thermal quenching that had to be accounted for. Uranine sorption was insignificant after fluorescence and concentration correction at low concentrations of 0.5 and 5 $\mu g\ L^{-1}$, became weakly sorptive at 20 $\mu g\ L^{-1}$ and significantly sorptive at 50 $\mu g\ L^{-1}$ with little dependence on temperature.

The dataset and methodology presented in this thesis work provide a site-specific dataset as well as a framework for future uranine tracer test interpretation in fractured crystalline aquifers. Temperature-specific fluorometric analysis was necessary to account for changes in fluorescence intensity with temperature, showing that in this environment

concentration and fluorescence correction dominate over temperature alone to explain measured tracer response.

7. Future Work

Future research should focus on testing whether the batch-scale findings obtained in this study are transferable to field conditions in fractured gneiss aquifers. In particular, controlled field tracer tests combined with breakthrough-curve analysis are needed to assess whether incomplete recovery and late-time tailing can be explained solely by physical transport processes such as fracture-matrix exchange, or whether weak chemical retention of uranine also contributes under higher tracer concentrations.

To support this interpretation, transport modelling should be undertaken to link the laboratory batch results with field-scale tracer behaviour. Coupled modelling approaches that incorporate advection, dispersion, matrix exchange, and concentration-dependent sorption would help clarify the relative importance of physical and chemical controls on uranine transport in crystalline aquifers [11].

Further laboratory studies should also investigate longer equilibration times, larger replicate numbers, and experimental designs that better approximate natural fracture conditions, including intact rock surfaces or flow-through systems [11]. In addition, future work should examine the influence of particle size and reactive surface area more explicitly since these factors may affect the apparent extent of sorption in crushed-rock experiments. This would improve the comparability of laboratory studies and strengthen the interpretation of tracer behavior in the field.

Finally, future applications of uranine in crystalline-rock tracer studies should continue to use matrix-matched, temperature-specific calibration procedures so that fluorescence quenching is not misinterpreted as tracer loss by sorption.

8. Conclusion

The temperature dependence of uranine transport behavior in groundwater and gneiss from the Freiberg fractured aquifer was characterized to distinguish actual tracer retention from apparent tracer loss due to fluorescence quenching.

Results reveal that fluorescence remains strongly and approximately linearly related to concentration across all experimental temperatures; however, it is strongly affected by temperature changes and therefore requires a matrix-matched, temperature-dependent calibration.

Detectable sorption was absent at concentrations of 0.5 and 5 µg/L after calibration, but weakly positive sorption emerged at 20 µg/L and strengthened further at 50 µg/L.

Sorption itself proved only modestly and non-monotonically temperature-dependent compared to fluorescence yield. Mild water-rock interaction during the batch experiments is indicated by small but systematic shifts in dissolved major ions, while pH and carbonate hardness remained mostly unchanged.

The main implication of this study is therefore methodological in addition to hydrogeochemical. It found that fluorescence detection, and not sorption behaviour, is affected more strongly by temperature in this fractured gneiss system. Concentration has a greater impact on uranine retention than temperature does. Uranine moves conservatively under low concentration, typical of many tracer tests in the field in the Freiberg groundwater-gneiss system but should not be considered perfectly conservative at higher concentrations.

Following this, two practical recommendations can be made for future tracer use in crystalline aquifers. Firstly, uranine concentrations should be quantified using matrix-matched calibration that accounts for temperature conditions relevant to the tracer test. Secondly, apparent incomplete recovery or late-time tailing in fluorescent dye tracer tests should not be ascribed solely to fracture-matrix exchange or immobile-porosity effects at high tracer concentrations, because weak chemical retention may additionally play a role.

References

1. Abdelaziz R, Merkel BJ. Sensitivity analysis of transport modeling in a fractured gneiss aquifer. Journal of African Earth Sciences. 2015 Mar 1;103:121–7. doi:10.1016/j.jafrearsci.2014.12.003
2. Goldscheider N, Meiman J, Pronk M, Smart C. Tracer tests in karst hydrogeology and speleology. International Journal of Speleology [Internet]. Available from: www.ijs.speleo.it
3. Weidner C. Parameters affecting Na-fluorescein (uranine) detection in mine water tracer tests. Mine Water – Managing the Challenges. 2011.
4. Sabatini DA. Sorption and intraparticle diffusion of fluorescent dyes with consolidated aquifer media. Ground Water. 2000;38(5):651–6. doi:10.1111/j.1745-6584.2000.tb02700.x
5. Blaen PJ, Brekenfeld N, Comer-Warner S, Krause S. Multitracer Field Fluorometry: Accounting for Temperature and Turbidity Variability During Stream Tracer Tests. Water Resour Res. 2017 Nov 1;53(11):9118–26. doi:10.1002/2017WR020815
6. Bork M, Lange J, Graf-Rosenfellner M, Lang F. Controls of fluorescent tracer retention by soils and sediments [Internet]. 2018. Available from: https://hess.copernicus.org/preprints/hess-2018-549/ doi:10.5194/hess-2018-549
7. Vaitl T, Wohnlich S. Batch-experiments for the determination of sorption and reaction kinetics of fluorescent dyes. Grundwasser. 2018 Jun 1;23(2):141–53. doi:10.1007/s00767-018-0390-7
8. Leibundgut C, Maloszewski P, Külls C. Tracers in hydrology. Wiley-Blackwell; 2009. 415 p.
9. Abdul AS, Gibson TL. Equilibrium Batch Experiments with Six Polycyclic Aromatic Hydrocarbons and Two Aquifer Materials. HAZARDOUS WASTE & HAZARDOUS MATERIALS. Mary Ann Liebert, Inc., Publishers; 1986.
10. OECD. OECD Guideline for the Testing of Chemicals: Adsorption-Desorption Using a Batch Equilibrium Method. OECD Test Guideline 106.
11. Lakowicz JR. Principles of Fluorescence Spectroscopy. 3rd ed. Springer.
12. Baker A. Thermal fluorescence quenching properties of dissolved organic matter. Water Res. 2005;39(18):4405–12. doi:10.1016/j.watres.2005.08.023 PubMed PMID: 16213540.
13. Weidner C. IMWA2011_Weidner_327. International Mine Water Association Congress; 2011.

14. Luchowski R, Sabnis S, Szabelski M, Sarkar P, Raut S, Gryczynski Z, et al. Self-quenching of uranin: Instrument response function for color sensitive photo-detectors. J Lumin. 2010 Dec;130(12):2446–51. doi:10.1016/j.jlumin.2010.07.027

15. Magal E, Weisbrod N, Yakirevich A, Yechieli Y. The use of fluorescent dyes as tracers in highly saline groundwater. J Hydrol (Amst). 2008 Aug 30;358(1–2):124–33. doi:10.1016/j.jhydrol.2008.05.035

16. Abdelaziz R, Merkel BJ. Analytical and Numerical Modeling of Flow in a Fractured Gneiss Aquifer. J Water Resour Prot. 2012;04(08):657–62. doi:10.4236/jwarp.2012.48076

17. Abdelaziz R, Pearson AJ, Merkel BJ. Lattice Boltzmann modeling for tracer test analysis in a fractured Gneiss aquifer. Nat Sci (Irvine). 2013;05(03):368–74. doi:10.4236/ns.2013.53050

18. Vasu D, Singh S, Tiwary P, Sahu N, Ray SK, Butte PS, et al. Influence of geochemical processes on hydrochemistry and irrigation suitability of groundwater in part of semi-arid Deccan Plateau, India. Appl Water Sci. 2017;7(7):3803-15. doi:10.1007/s13201-017-0528-2.1

19. Ryu JS, Jacobson AD, Holmden C, Lundstrom CC, Zhang Z. The major ion, δ44/40Ca, δ44/42Ca, and δ26/24Mg geochemistry of granite weathering at pH=1 and T=25 °C: power-law processes and the relative reactivity of minerals. Geochim Cosmochim Acta. 2011;75(20):6004-26. doi:10.1016/j.gca.2011.07.025.2

20. Schwientek M, Einsiedl F, Stichler W, Stögbauer A, Strauß H, Małoszewski P. Evidence for denitrification regulated by pyrite oxidation in a heterogeneous porous groundwater system. Chem Geol. 2008;255(1-2):60-7. doi: 10.1016/j.chemgeo.2008.06.005.3

21. Jørgensen CJ, Jacobsen OS, Elberling B, Aamand J. Microbial oxidation of pyrite coupled to nitrate reduction in anoxic groundwater sediment. Environ Sci Technol. 2009;43(13):4851-7. doi:10.1021/es803417s.4

22. Banwart SA, Evans KA, Croxford S. Predicting mineral weathering rates at field scale for mine water risk assessment. Geol Soc Lond Spec Publ. 2002;198(1):137-57. doi:10.1144/GSL.SP.2002.198.01.10.5

23. Granato GE, DeSimone LA, Barbaro JR, Jeznach LC. Methods for evaluating potential sources of chloride in surface waters and groundwaters of the conterminous United States. Reston (VA): U.S. Geological Survey; 2015. Open-File Report 2015-1080. doi:10.3133/ofr20151080.

Appendix A

A.1 Mean (± 1 SD) anion concentrations in batch reactor samples — Ion Chromatography (IC)

n = 3 replicates per condition. '<DL' = all replicates below detection limit (excluded from mean/SD). Chloride and Sulfate: 1:5 dilution applied and corrected.

Temp. (°C)	Initial Uranine (µg/L)	Matrix	n	Bromide (mg/L)	Nitrate (mg/L)	Chloride (mg/L)	Sulfate (mg/L)
10	0.5	Water + Tracer	3	0.38 ± 0.00	18.27 ± 0.15	209.93 ± 0.46	105.80 ± 0.56
10	0.5	Water + Tracer + Gneiss	3	0.38 ± 0.00	18.92 ± 0.06	218.07 ± 1.24	121.67 ± 6.62
10	50.0	Water + Tracer	3	0.38 ± 0.01	18.48 ± 0.14	210.80 ± 0.10	106.20 ± 0.89
10	50.0	Water + Tracer + Gneiss	3	0.38 ± 0.00	19.13 ± 0.12	228.07 ± 6.44	120.43 ± 0.42
10	–	–	3	0.38 ± 0.00	18.48 ± 0.06	211.47 ± 0.35	106.03 ± 0.15
25	0.5	Water + Tracer	3	0.34 ± 0.00	18.19 ± 0.90	212.00 ± 0.87	107.07 ± 0.38
25	0.5	Water + Tracer + Gneiss	3	0.35 ± 0.00	18.85 ± 0.29	222.43 ± 3.48	120.33 ± 1.68
25	50.0	Water + Tracer	3	0.35 ± 0.01	18.40 ± 0.23	214.77 ± 2.68	108.63 ± 1.42
25	50.0	Water + Tracer + Gneiss	3	0.35 ± 0.00	18.92 ± 0.42	226.37 ± 8.35	121.53 ± 4.01
25	–	–	3	0.35 ± 0.00	18.14 ± 0.57	213.67 ± 1.18	107.67 ± 0.45
55	0.5	Water + Tracer	3	0.34 ± 0.00	18.96 ± 0.25	217.87 ± 8.35	107.07 ± 1.27
55	0.5	Water + Tracer + Gneiss	3	0.35 ± 0.00	19.48 ± 0.04	221.03 ± 4.50	121.20 ± 3.20
55	50.0	Water + Tracer	3	0.34 ± 0.01	18.84 ± 0.37	211.83 ± 1.69	107.13 ± 0.93
55	50.0	Water + Tracer + Gneiss	3	0.35 ± 0.01	18.85 ± 0.46	224.27 ± 5.71	121.37 ± 1.81
55	–	–	3	0.34 ± 0.00	18.64 ± 0.34	211.40 ± 1.39	106.77 ± 0.90

A2. Mean (± 1 SD) major cation concentrations in batch reactor samples — Ion Chromatography (IC)

n = 3 replicates per condition. 1:2 dilution applied and corrected

Temp. (°C)	Initial Uranine (µg/L)	Matrix	n	Na (mg/L)	K (mg/L)	Mg (mg/L)	Ca (mg/L)
10	0.5	Water + Tracer	3	56.45 ± 0.06	5.32 ± 0.06	26.39 ± 0.09	89.85 ± 0.26
10	0.5	Water + Tracer + Gneiss	3	59.23 ± 0.63	11.13 ± 0.18	28.09 ± 0.08	95.75 ± 0.90
10	50.0	Water + Tracer	3	56.76 ± 0.20	5.30 ± 0.04	26.44 ± 0.05	90.47 ± 0.72
10	50.0	Water + Tracer + Gneiss	3	66.13 ± 4.81	11.82 ± 0.31	28.80 ± 0.12	99.12 ± 0.97
10	–	–	3	57.03 ± 0.17	5.40 ± 0.12	26.56 ± 0.12	90.39 ± 0.38
25	0.5	Water + Tracer	3	58.15 ± 0.54	5.38 ± 0.04	26.86 ± 0.07	91.38 ± 0.38
25	0.5	Water + Tracer + Gneiss	3	60.02 ± 1.63	12.63 ± 0.20	28.60 ± 0.16	99.10 ± 1.90
25	50.0	Water + Tracer	3	58.09 ± 0.24	5.25 ± 0.21	26.95 ± 0.08	91.69 ± 0.43
25	50.0	Water + Tracer + Gneiss	3	62.97 ± 4.70	12.25 ± 0.21	28.62 ± 0.02	98.70 ± 1.79
25	–	–	3	58.15 ± 0.27	5.39 ± 0.03	26.97 ± 0.04	91.77 ± 0.13
55	0.5	Water + Tracer	3	58.03 ± 0.11	5.60 ± 0.16	27.05 ± 0.08	91.75 ± 0.08
55	0.5	Water + Tracer + Gneiss	3	62.47 ± 2.61	11.70 ± 0.17	27.63 ± 0.21	100.19 ± 1.32
55	50.0	Water + Tracer	3	58.49 ± 0.46	5.43 ± 0.02	27.17 ± 0.02	92.34 ± 0.10
55	50.0	Water + Tracer + Gneiss	3	63.31 ± 2.75	12.10 ± 0.41	27.79 ± 0.39	100.44 ± 1.10
55	–	–	3	58.18 ± 0.47	5.39 ± 0.06	27.12 ± 0.05	92.28 ± 0.31

A3. Mean (± 1 SD) trace element concentrations in batch reactor samples — ICP-OES (µg/L)

n = 3 replicates per condition. Only elements with ≥ 1 detectable value shown; elements below detection in all samples (Ag, As, Bi, Cd, Cr, Ga, In, Pb, Tl) omitted. ICP-OES data available for 0.5 and 50 µg/L uranine concentrations only. Shading: blue = 10 °C | green = 25 °C | yellow = 55 °C.

Temp. (°C)	Initial Uranine (µg/L)	Matrix	n	Al (µg/L)	Ba (µg/L)	Co (µg/L)	Cu (µg/L)	Fe (µg/L)	Mn (µg/L)	Ni (µg/L)	Sr (µg/L)	Zn (µg/L)
10	0.5	Water + Tracer	3	<DL	43.53 ± 0.23	<DL	<DL	19.40	9.71 ± 1.64	10.80 ± 0.20	466.67 ± 3.21	73.47 ± 0.45
10	0.5	Water + Tracer + Gneiss	3	<DL	56.23 ± 0.84	<DL	<DL	<DL	340.67 ± 49.22	10.23 ± 1.70	427.33 ± 6.11	<DL
10	50	Water + Tracer	3	<DL	43.67 ± 0.06	<DL	<DL	90.45 ± 84.22	10.60 ± 1.28	10.80 ± 0.40	461.67 ± 1.53	71.93 ± 1.42
10	50	Water + Tracer + Gneiss	3	<DL	72.97 ± 4.82	9.84 ± 2.80	<DL	298.00	662.00 ± 27.84	25.97 ± 4.75	454.67 ± 3.21	13.89 ± 5.66
10	B	Blank (water only)	3	<DL	43.60 ± 0.53	<DL	<DL	<DL	8.58 ± 0.24	10.33 ± 0.35	468.00 ± 7.94	72.70 ± 1.01
25	0.5	Water + Tracer	3	<DL	44.00 ± 0.53	<DL	<DL	<DL	9.24 ± 0.54	10.80 ± 0.35	474.33 ± 8.14	75.97 ± 2.34
25	0.5	Water + Tracer + Gneiss	3	<DL	76.87 ± 2.64	6.23 ± 0.39	<DL	68.20	721.67 ± 59.69	17.03 ± 1.15	451.33 ± 13.05	7.00 ± 1.30
25	50	Water + Tracer	3	<DL	43.67 ± 0.21	<DL	5.75	50.50	8.89 ± 0.33	10.60 ± 0.17	463.00 ± 1.73	75.80 ± 1.81
25	50	Water + Tracer + Gneiss	3	34.40	66.70 ± 3.06	<DL	<DL	91.50	504.67 ± 63.41	8.78 ± 1.24	433.00 ± 16.70	6.50 ± 0.37
25	B	Blank (water only)	3	<DL	43.13 ± 0.31	<DL	<DL	<DL	8.88 ± 0.35	10.67 ± 0.06	462.33 ± 2.31	84.50 ± 20.46
55	0.5	Water + Tracer	3	<DL	43.37 ± 0.06	<DL	<DL	21.90 ± 4.53	9.29 ± 0.34	10.67 ± 0.25	463.67 ± 3.21	74.40 ± 2.63
55	0.5	Water + Tracer + Gneiss	3	<DL	76.03 ± 1.37	<DL	<DL	<DL	260.67 ± 23.44	<DL	422.67 ± 4.04	<DL
55	50	Water + Tracer	3	<DL	43.43 ± 0.42	<DL	<DL	<DL	9.45 ± 0.19	10.07 ± 0.65	463.00 ± 1.73	70.27 ± 1.19

55	50	Water + Tracer + Gneiss	3	<DL	82.77 ± 8.56	<DL	<DL	20.40	286.67 ± 46.36	5.36	431.33 ± 4.51	<DL
55	B	Blank (water only)	3	<DL	43.60 ± 0.78	<DL	<DL	<DL	8.63 ± 0.30	10.21 ± 0.29	470.67 ± 7.51	65.97 ± 8.60

Appendix B

B.1 Full batch-sorption dataset

The complete batch-sorption dataset from which the summary statistics in Table 3 were derived is reproduced in Table 5. Each temperature–concentration cell contains three replicate WTG reactor measurements together with the paired WT control values used to establish matrix-matched calibration. Reported quantities include raw fluorescence-derived WTG and WT intensities, the mean initial concentration c_0, the equilibrium concentration c_{eq}, the calculated sorbed amount q, sorption percentage, and the apparent distribution coefficient K_d. Triplicate-group statistics are reported alongside: mean q, standard deviation, standard error, the one-sample t-statistic against the null hypothesis $q = 0$, the critical t-value ($t_{crit} = 4.303$ for $n = 3$ replicates at $\alpha = 0.05$), the resulting 95 % confidence-interval half-width Δq, and the lower and upper 95 % confidence bounds. Replicate values of the sorbed amount q (µg g^{-1}), sorption percentage, distribution coefficient K_d (L kg^{-1}), standard deviation, standard error, t-statistic, t-critical (4.303 for n = 3), Δq (margin of error) and 95 % confidence interval (lower, upper limits) for every temperature–concentration combination.

T (°C)	C (µg/L)	Intensity (WTG)	Intensity (WT)	c_0 µg/L)	c_{eq} µg/L)	q (µg g^{-1})	Sorp %	K_d (L/kg)	Mean q	Standard deviation q	SE	t	Δq	Lower	Upper
10	0.5	4.790	2.299	0.45	0.972	−0.0016	−1.16	−0.00162	−0.0020	0.000615	0.000355	−5.572	0.00153	−0.0035	−0.0005
		6.812	2.347		1.344	−0.0027	−1.99	−0.00200							
		4.988	2.235		1.009	−0.0017	−1.24	−0.00167							

T (°C)	C (µg/L)	Intensity (WTG)	Intensity (WT)	c_0 µg/L)	c_{eq} µg/L)	q (µg g^{-1})	Sorp %	K_d (L/kg)	Mean q	Standard deviation q	SE	t	Δq	Lower	Upper
	5	43.046	31.581	5.06	7.994	−0.0088	−0.58	−0.00110	−0.0012	0.00664	0.00383	−0.302	0.01648	−0.0176	0.0153
		22.500	30.734		4.223	0.0025	0.17	0.00060							
		21.936	21.942		4.119	0.0028	0.19	0.00069							
	20	87.416	94.223	19.99	16.137	0.0116	0.19	0.00072	0.0117	0.00150	0.000863	13.508	0.00371	0.0079	0.0154
		84.512	108.034		15.604	0.0132	0.22	0.00085							
		89.924	127.327		16.598	0.0102	0.17	0.00061							
	50	249.846	414.355	76.12	45.949	0.0907	0.40	0.00197	0.0895	0.00435	0.00251	35.646	0.01080	0.0787	0.1003
		260.801	424.065		47.960	0.0847	0.37	0.00177							
		245.511	405.483		45.153	0.0931	0.41	0.00206							
25	0.5	8.353	2.347	1.50	2.308	−0.0024	−0.54	−0.00105	−0.0066	0.00861	0.00497	−1.321	0.02137	−0.0279	0.0148
		41.890	3.080		6.976	−0.0165	−3.64	−0.00236							
		4.497	2.326		1.771	−0.0008	−0.18	−0.00046							
	5	29.047	29.847	5.35	5.188	0.0005	0.03	0.000095		0.000612					0.0013

T (°C)	C (µg/L)	Intensity (WTG)	Intensity (WT)	c_0 µg/L)	c_{eq} µg/L)	q (µg g^{-1})	Sorp %	K_d (L/kg)	Mean q	Standard deviation q	SE	t	Δq	Lower	Upper
		31.579	30.642		5.541	−0.0006	−0.04	−0.000102	−0.0002		0.000353	−0.601	0.00152	−0.0017	
		31.580	30.202		5.541	−0.0006	−0.04	−0.000102							
	20	108.903	122.352	17.98	16.303	0.0050	0.09	0.00031	0.0048	0.00153	0.000885	5.418	0.00381	0.0010	0.0086
		106.181	120.437		15.924	0.0062	0.11	0.00039							
		113.430	120.102		16.933	0.0032	0.06	0.00019							
	50	336.773	339.855	50.82	48.020	0.0084	0.06	0.000175	0.0115	0.00324	0.00187	6.133	0.00803	0.0034	0.0195
		321.388	366.883		45.878	0.0149	0.10	0.000324							
		330.355	364.490		47.126	0.0111	0.07	0.000235							
55	0.5	4.990	4.417	1.69	1.727	−0.0001	−0.02	-6.3×10^{-5}	−0.0001	0.000105	6.06×10^{-5}	−1.800	0.000261	−0.0004	0.0002
		5.267	4.700		1.761	−0.0002	−0.04	-1.2×10^{-4}							
		4.711	5.002		1.692	0.0000	0.00	-2.4×10^{-6}							
	5	26.848	33.819	5.50	4.469	0.0031	0.19	0.000695		0.00686	0.00396				0.0155

T (°C)	C (µg/L)	Intensity (WTG)	Intensity (WT)	c_0 µg/L)	c_{eq} µg/L)	q (µg g^{-1})	Sorp %	K_d (L/kg)	Mean q	Standard deviation q	SE	t	Δq	Lower	Upper
		59.941	34.013		8.622	−0.0094	−0.57	−0.00109	−0.0015			−0.377	0.01704	−0.0185	
		30.334	37.545		4.907	0.0018	0.11	0.000365							
	20	108.501	145.409	17.52	14.715	0.0084	0.16	0.000573	0.0103	0.00169	0.000978	10.560	0.00421	0.0061	0.0145
		102.054	124.606		13.906	0.0109	0.21	0.000781							
		99.868	123.630		13.631	0.0117	0.22	0.000857							
	50	304.034	412.593	51.04	39.249	0.0354	0.23	0.000903	0.0417	0.00596	0.00344	12.112	0.01480	0.0269	0.0565
		272.559	388.385		35.299	0.0473	0.31	0.00134							
		285.910	393.355		36.975	0.0423	0.28	0.00114							

Appendix C

C.1 Field parameters in WT and WTG reactors

Carbonate hardness, pH, EC, temperature at measurement in WT and WTG reactors at each experimental temperature and nominal uranine concentration. Values are triplicate means.

Temperature (°C)	Concentration (µg L^{-1})	Carbonate hardness(°d)		pH		pH Temperature (°C)		Electric conductivity (µS cm^{-1})		EC temperature (°C)	
		WTG	WT	WTG	WT	WTG	WT	WTG	WT	WTG	WT
10	0	1.80		6.42		20.23		1043.33		20.13	
	0.5	3.00	1.77	6.93	6.71	19.00	19.67	1124.67	1042.67	18.50	19.13
	5	2.80	1.77	6.52	6.56	20.13	19.23	1143.00	1033.67	19.83	19.47
	20	2.93	1.80	6.59	6.51	19.70	20.03	1089.00	1040.00	19.57	19.60
	50	2.70	1.60	6.99	6.68	17.80	19.53	1103.00	1037.00	17.40	19.23
20	0.5	2.90	1.53	6.35	6.62	20.23	20.10	1136.00	1036.33	19.93	19.97
	50	2.60	1.40	6.59	6.66	20.47	20.00	1115.00	1041.00	20.03	19.70
55	0.5	2.25	1.50	7.04	7.12	20.37	19.77	1129.33	1129.00	20.90	19.40
	50	2.60	1.57	7.11	7.25	20.40	20.23	1310.33	1073.33	19.93	19.90